haematologica
Journal of The Ferrata Storti Foundation

Glutathione peroxidase 4 and vitamin E control reticulocyte maturation, stress erythropoiesis and iron homeostasis

by Sandro Altamura, Naidu M. Vegi, Philipp S. Hoppe, Timm Schroeder, Michaela Aichler, Axel Walch, Katarzyna Okreglicka, Lothar Hültner, Manuela Schneider, Camilla Ladinig, Cornelia Kuklik-Roos, Josef Mysliwietz, Dirk Janik, Frauke Neff, Birgit Rathkolb, Martin Hrabé de Angelis, Christian Buske, Ana Rita da Silva, Katja Muedder, Marcus Conrad, Tomas Ganz, Manfred Kopf, Martina U. Muckenthaler, and Georg W. Bornkamm

Haematologica 2019 [Epub ahead of print]

Citation: Sandro Altamura, Naidu M. Vegi, Philipp S. Hoppe, Timm Schroeder, Michaela Aichler, Axel Walch, Katarzyna Okreglicka, Lothar Hültner, Manuela Schneider, Camilla Ladinig, Cornelia Kuklik-Roos, Josef Mysliwietz, Dirk Janik, Frauke Neff, Birgit Rathkolb, Martin Hrabé de Angelis, Christian Buske, Ana Rita da Silva, Katja Muedder, Marcus Conrad, Tomas Ganz, Manfred Kopf, Martina U. Muckenthaler, and Georg W. Bornkamm. Glutathione peroxidase 4 and vitamin E control reticulocyte maturation, stress erythropoiesis and iron homeostasis. Haematologica. 2019; 104:xxx doi:10.3324/haematol.2018.212977

Glutathione peroxidase 4 and vitamin E control reticulocyte maturation, stress erythropoiesis and iron homeostasis

Sandro Altamura[1,2,*], Naidu M. Vegi[3,*], Philipp S. Hoppe[4], Timm Schroeder[4], Michaela Aichler[5], Axel Walch[5], Katarzyna Okreglicka[6], Lothar Hültner[7], Manuela Schneider[8], Camilla Ladinig[7], Cornelia Kuklik-Roos[7], Josef Mysliwietz[9], Dirk Janik[5], Frauke Neff[5], Birgit Rathkolb[10-12], Martin Hrabé de Angelis[11-13], Christian Buske[3], Ana Rita da Silva[1,2],Katja Muedder[1,2], Marcus Conrad[14], Tomas Ganz[15], Manfred Kopf[6], Martina U. Muckenthaler[1,2], Georg W. Bornkamm[7,#]

[1] Department of Pediatric Hematology, Oncology and Immunology - University of Heidelberg, INF 350, D-69120 Heidelberg, Germany

[2] Molecular Medicine Partnership Unit, Heidelberg, Germany

[3] Institute of Experimental Cancer Research, Universitätsklinikum Ulm, Albert-Einstein-Allee 23, 89081 Ulm, Germany

[4] Department of Biosystems Bioscience and Engineering, ETH Zürich, Mattenstrasse 26, 4058 Basel, Switzerland

[5] Research Unit Analytical Pathology, Helmholtz Zentrum München, Deutsches Forschungszentrum für Gesundheit und Umwelt (GmbH), 85764 Neuherberg, Germany

[6] Institute of Molecular Health Sciences, ETH Zurich, 8093 Zürich, Switzerland

[7] Institute of Clinical Molecular Biology and Tumor Genetics, Helmholtz Zentrum München, Deutsches Forschungszentrum für Gesundheit und Umwelt (GmbH), Marchioninistr. 25, D-81377 München, Germany

[8] Institute for Stroke and Dementia Research (ISD), Klinikum der Universität München, Feodor-Lynen-Straße 17, 81377 München, Germany

[9] Institute of Molecular Immunology, Helmholtz Zentrum München, Deutsches Forschungszentrum für Gesundheit und Umwelt (GmbH), Marchioninistr. 25, D-81377 München, Germany

[10] Institute of Molecular Animal Breeding and Biotechnology, Ludwig-Maximilians-Universität München, Genzentum, Feodor-Lynen-Str.25, 81377 München, Germany

[11] Institute of Experimental Genetics, Geman Mouse Clinic (GMC), Helmholtz Zentrum München, Deutsches Forschungszentrum für Gesundheit und Umwelt (GmbH), 85764 Neuherberg, Germany

[12] German Center for Diabetes Research (DZD), Ingolstädter Landstr. 1, 85764 Neuherberg, Germany

[13] Chair of Experimental Genetics, School of Life Science Weihenstephan, Technische Universität München, Alte Akademie 8, 85354 Freising, Germany

[14] Institute of Developmental Genetics, Helmholtz Zentrum München, Deutsches Forschungszentrum für Gesundheit und Umwelt (GmbH), 85764 Neuherberg, Germany

[15] Departments of Medicine and Pathology, David Geffen School of Medicine, UCLA, Los Angeles, USA

*These authors contributed equally to this work

[#]To whom correspondence should be addressed: georg.bornkamm@t-online.de

Running title: GPX4 controls reticulocyte maturation

ABSTRACT

Glutathione peroxidase 4 (GPX4) is unique as it is the only enzyme that can prevent detrimental lipid peroxidation in vivo by reducing lipid peroxides to the respective alcohols thereby stabilizing oxidation products of unsaturated fatty acids. During reticulocyte maturation, 15-lipoxygenase-mediated lipid peroxidation in humans and rabbits and by 12/15-lipoxygenase (ALOX15) in mice had been considered as the initiating event for the elimination of mitochondria which is now known to occur through mitophagy. Yet, genetic ablation of the *Alox15* gene in mice failed to provide evidence for this hypothesis. We designed a different genetic approach to tackle this open conundrum. Since either other lipoxygenases or non-enzymatic autooxidative mechanisms may compensate for the loss of *Alox15*, we asked whether ablation of *GPX4* in the hematopoietic system would result in perturbation of reticulocyte maturation. Quantitative assessment of erythropoiesis indices in the blood, bone marrow and spleen of chimeric mice with *GPX4* ablated in hematopoietic cells revealed anemia with an increase in the fraction of erythroid precursor cells and reticulocytes. Additional dietary vitamin E depletion strongly aggravated the anemic phenotype. Despite strong extramedullary erythropoiesis reticulocytes failed to mature and accumulated large autophagosomes with engulfed mitochondria. *GPX4*-deficiency in hematopoietic cells led to systemic hepatic iron overload and simultaneous severe iron demand in the erythroid system. Despite extremely high erythropoietin and erythroferrone levels in the plasma, hepcidin expression remained unchanged. Conclusively, perturbed reticulocyte maturation in response to *GPX4* loss in hematopoietic cells thus causes ineffective erythropoiesis, a phenotype partially masked by dietary vitamin E supplementation.

INTRODUCTION

Glutathione peroxidase 4 (GPX4) is unique in its ability to reduce lipid peroxidation products in biological membranes in vivo.[1,2] Lipid peroxidation is brought about either enzymatically by lipoxygenases at specific sites or unselectively by non-enzymatic mechanisms, usually through Fe^{2+}-driven Fenton chemistry.[3] Lipoxygenases are dioxygenases that catalyze the incorporation of molecular oxygen into polyunsaturated fatty acids (PUFA) in a site- and stereospecific manner thus yielding the respective hydroxyperoxides. Lipoxygenases become activated by low concentrations of peroxides (the so called “peroxide tone”) that oxidize Fe^{2+} to Fe^{3+} in the catalytic site.[4] The peroxide tone and the activity of lipoxygenases is under the control GPX4. 12/15-Lipoxygenase and GPX4 act antagonistically as far as oxidation (lipoxygenases) and reduction (GPX4) of substrates, and induction of cell death and cell survival are concerned. 12/15-lipoxygenase induces cell death in murine fibroblasts, whereas GPX4 rescues cells from lipoxygenase-induced cell death.[5] But in other settings, lipoxygenases and GPX4 biochemically cooperate: lipoxygenases generate highly reactive peroxidation products of unsaturated fatty acids (P-O-O-H) that are prone to further uncontrolled lipid membrane peroxidation. GPX4 reduces these peroxides to stable hydroxyl-derivatives (P-O-H).[6-9] Thereby, 15-lipoxygenase in humans or 12/15-lipoxygenase, its functional homolog in mice, and GPX4 constitute a pair of enzymes whose activities are tightly interconnected.[5,9] In the interplay of lipoxygenases and GPX4 the role of vitamin E also has to be considered. Vitamin E intercalates into membranes, acts as a chain breaker of lipid peroxidation through its high affinity for unpaired electrons and thus antagonizes peroxide production.

GPX4 is one of 24 (25 in man) selenoproteins in mammals[10] and is positioned at the top of the hierarchy of selenoproteins, i.e. GPX4 expression is maintained even under severe selenium-deficiency when the synthesis of most other selenoproteins has ceased.[11] GPX4 has evolved to carry the 21st amino acid selenocysteine rather than its functional counterpart cysteine in the active site which renders the enzyme highly resistant to irreversible overoxidation through peroxides.[12] Dietary selenium is known to be required for stress erythropoiesis in mice[13,14] and blockage of the synthesis of all selenoproteins in hematopoietic cells by selective deletion of the selenocysteine-specific t-RNA *Trsp* in the bone marrow of chimeric mice severely impairs stress erythropoiesis.[13]

Mitochondria are removed from reticulocytes by a particular form of autophagy, called mitophagy,[15,16] and oxidized lipids are considered to play a crucial role in triggering autophagy in various cell types.[17,18] Furthermore, macrophages from 12/15-lipoxygenase

knockout mice exhibit abnormal mitochondria, cytoplasmic vacuoles and an altered phospholipidomics pattern indicative of impaired autophagy.[19] In addition, the 12/15-lipoxygenase oxidation product 12-hydroxyeicosatetraenoic acid-phosphatidylethanolamine (12-HETE-PE) was shown to be a better substrate for yeast Atg8 than native PE, whereas native as well as oxidized PE were both effective substrates for LC3 lipidation. With regard to reticulocyte maturation current data suggest that elimination of mitochondria through mitophagy may be stimulated by oxidation products of polyunsaturated membrane phospholipids.

15-lipoxygenase is highly expressed in reticulocytes and was reported to be involved in the elimination of mitochondria by Rapoport and his coworkers.[20-23] The initial work of the Rapoport group was confirmed and extended by van Leyen et al. who reported a similar 12/15-lipoxygenase-driven mechanism that degrades organelles in the eye lens.[24,25] Yet, the great interest in this early work decreased with the findings that erythrocyte and reticulocyte counts were normal in 12/15-lipoxygenase knockout mice.[26] Definitive genetic proof for a role of lipid oxidation during reticulocyte maturation is thus still lacking. Several reasons may account for the fact that 12/15-lipoxygenase knockout mice exhibit normal red blood and reticulocyte counts: (i) lipoxygenases other than 12/15-lipoxygenase may compensate for the targeted loss of reticulocyte 12/15-lipoxygenase; (ii) lipoxygenases may become dispensable if non-enzymatic mechanisms of lipid oxidation prevail[27-29]; or (iii) lipid oxidation events are dispensable during reticulocyte maturation.

Our present work was conceived to provide a definitive answer as to whether lipid oxidation is indeed critically involved in mitophagy in reticulocytes using a well-defined genetic approach. Whereas many different enzymatic and non-enzymatic mechanisms may account for the initial lipid oxidation step, GPX4 stands out as the only enzyme that effectively prevents detrimental lipid peroxidation and allows lipid oxidation to proceed in a highly controlled manner. Thus, if lipid oxidation is an essential step in the elimination of mitochondria in reticulocytes, ablation of *GPX4* should result in uncontrolled lipid peroxidation and perturbation of reticulocyte maturation. Since GPX4 is essential for early embryonic development and the survival of adult mice,[30,31] *GPX4* had to be deleted specifically in hematopoietic cells. To this end, we took advantage of the Tamoxifen-inducible Cre/lox system [32], which is of invaluable help when the side effects of Cre[33-37] and Cre activators[38] or inducers[39] are properly controlled. We show that GPX4 is required for stress erythropoiesis. Deletion of *GPX4* in adult mice causes anemia and ineffective erythropoiesis due to impaired reticulocyte maturation, a phenotype dramatically aggravated

by depleting vitamin E from the diet. As a consequence hepatic iron overload develops despite the continuous iron demand for red blood cell production.

METHODS

Mice

Mice were bred under SPF conditions. *GPX4$^{fl/fl}$;CreERT2* mice were backcrossed for at least ten generations onto C57BL/6J mice (Taconic Biosciences, Köln, Germany). All animal experiments were performed according to the institutional guidelines and were approved by the local ethic committees on animal experimentation and by the Government of Upper Bavaria and Kantonales Veterinäramt in Zürich, respectively.

Generation of chimeric mice with GPX4-proficient and GPX4-deficient hematopoietic cells and analysis of blood parameters

Female wt recipient mice of 10 to 12 weeks (Taconic Biosciences, Köln) were lethally irradiated with 850 cGy and reconstituted with 10^6 bone marrow (BM) cells from *GPX4$^{fl/fl}$;CreERT2* or *GPX4$^{wt/wt}$;CreERT2* donor mice. BM cells had been collected by flushing the leg bones and crushing the pelvic bone. *GPX4$^{fl/fl}$; CreERT2* and *GPX4$^{wt/wt}$;CreERT2* mice have been described.[5,31,32] 150mg/kg 5-fluorouracil (FU) had been administered to donor mice by i.p. injection 24 hours prior to collecting BM cells from donor mice. After hematopoietic reconstitution mice were allowed to recover for 25 weeks. Mice were fed a tamoxifen citrate containing diet for three weeks following the protocol of Kiermayer *et al.*[40] to delete *GPX4*. EDTA-blood was collected from the tail vein before, at the last day of and at different time points after tamoxifen administration, and subjected to the analysis of blood parameters using a Sysmex XT-2000iV apparatus as described.[41]

Vitamin E depletion and repletion

Mice were deprived from vitamin E by feeding a vitamin E-depleted diet (SSNIFF, Soest, Germany) containing 7ppm α-tocopherol as compared to 55ppm in the normal diet. In initial experiments we have defined the conditions for ruling out side effects of Cre activation[33] with and without vitamin E-depletion using *GPX4$^{wt/wt}$;CreERT2* mice as controls (supplementary Fig.1). This allowed to apply a simplified protocol with C57BL/6J mice as controls and tamoxifen-treated, lethally irradiated wt mice reconstituted with BM cells of *GPX4$^{fl/fl}$;CreERT2* mice receiving a normal or a vitamin E-depleted diet as experimental groups (Fig.2-5,

supplementary Fig.5). The vitamin E-repleted diet (5x vitamin E) contained 275ppm α-tocopherol (SSNIFF, Soest, Germany).

Staining of erythroid precursor cells from bone marrow and spleen

Spleens were smashed and washed and the four leg bones flushed with 5mL PBS containing 1mM EDTA and 2%FCS. Cells were individualized, filtered through a 40µm cell strainer (BD Falcon) and incubated with 0.5µg anti-CD16/32 antibody in 50µl PBS for 30min on ice. BM cells were stained with 0.3µg CD44-PE-Cy7 (or CD71-PE-Cy7), 0.3µg Ter119-PE or Ter119-APC-Cy7 antibodies. Spleen cells were stained with the following lineage mix: each 0.5µg biotinylated CD3e (clone 145-2C11), CD11b (clone M1/70), CD19 (clone 1D3), B220 (clone RA3-6B2) and Gr-1 (clone RB6-8C5) antibodies. Cells were washed and stained with Streptavidin-Pacific Blue (Thermo Fisher) and 0.3µg CD71-PE-Cy7 and 0.3µg Ter119-PE (or Ter119-APC-Cy7) antibodies. Lineage-negative cells were gated and plotted as CD71-PE-Cy7- versus Ter119-APC-Cy7-positive cells. Cells were analysed on a FACSAriaI (Becton Dickinson).

Antibodies and Primers

See supplementary information.

RESULTS

GPX4-deficiency in hematopoietic cells impairs stress erythropoiesis

To study the role of GPX4 in hematopoiesis, chimeric mice were generated by reconstitution of lethally irradiated wt mice with *GPX4*$^{fl/fl}$*;Cre-ERT2* or *GPX4*$^{wt/wt}$*;Cre-ERT2* bone marrow (BM) cells. *GPX4* deletion in the hematopoietic system was induced by feeding tamoxifen citrate for 3 weeks.[40] At the last day of feeding tamoxifen red blood cell parameters and white blood cell counts (WBC) were significantly decreased and platelet indices increased in the experimental as well as in the control group revealing apparent Cre-mediated side effects[33] (supplementary Fig.1). Lymphocyte and monocyte counts were further decreased by simultaneous deletion of *GPX4* (supplementary Fig.1N-O).

Thus, the inducible activation of Cre-ERT2 by tamoxifen caused an aplastic anemia with a moderate decrease in red blood cell counts (RBC) presumably through induction of a DNA damage response regardless of the presence or absence of *GPX4* in hematopoietic cells. To separate a phenotype caused by *GPX4*-deficiency from that of Cre side effects, tamoxifen-

treated mice harboring *GPX4*$^{fl/fl}$*;Cre-ERT2* and *GPX4*$^{wt/wt}$*;Cre-ERT2* BM cells were allowed to recover and blood was drawn every three weeks (Fig.1). Mice with *GPX4*-deficient BM cells remained anemic with strongly elevated reticulocyte counts, whereas mice harboring *GPX4*$^{wt/wt}$*;Cre-ERT2* BM normalized their red blood parameters within 3 to 6 weeks (Fig.1E-H, additional RBC parameters in supplementary Fig.2B-F). Since recovery from anemia involves stress erythropoiesis,[42] *GPX4*-deficiency in the hematopoietic compartment thus impairs stress erythropoiesis. The erythropenic phenotype could be serially transplanted into lethally irradiated wt mice in two further rounds using *GPX4*-deficient BM donor cells. *GPX4*$^{fl/fl}$*;Cre-ERT2* mice served as controls except that tamoxifen feeding was omitted after the first transplantation (supplementary Fig.3). WBC and platelet parameters remained normal except for single outliers that were not reproduced during serial transplantation. The stable transmission of the erythropenic phenotype by serial transplantation is consistent with a marked defect in stress erythropoiesis, as hematopoietic reconstitution after lethal irradiation is driven by stress hematopoiesis.[43]

GPX4-deficient macrophages do not contribute to the development of erythropenia induced by deletion of GPX4 in the hematopoietic system

In our experimental strategy GPX4 was deleted in all hematopoietic cells including cells of the myeloid lineage. As macrophages are known to contribute to erythropoiesis by forming erythropoietic islands in the bone marrow,[44] it was important to discriminate whether erythropenia is brought about by a cell-autonomous effect of GPX4 on the erythroid lineage or by a cell-non-autonomous effect of GPX4 on macrophages. Liao et al. recently described that loss of all selenoproteins in hematopoietic cells by deletion of selenocysteine-specific t-RNA impairs stress erythropoiesis and have attributed this to the loss of selenoprotein W in macrophages[13]. Despite the high position of GPX4 in the hierarchy of selenoproteins, a cell-autonomous contribution of GPX4 to stress erythropoiesis was not considered by the authors.

To address a potential contribution of GPX4 in macrophages on stress erythropoiesis, we used GPX4$^{fl/fl}$;LysM-Cre mice that delete *GPX4* in macrophages and neutrophils[45] and analyzed bone marrow erythroblastic island macrophages (BMEIM) and spleen red pulp macrophages (RPM) by flow cytometry. The number of BMEIM was slightly reduced, while the number of RPM remained unaffected in the absence of GPX4 (supplementary Fig.4A-C). Importantly, erythrocyte and reticulocyte counts were unaltered as well as hemoglobin and

hematocrit values (Fig.1T-W) indicating that GPX4 in macrophages plays a minor if any role in the development of the erythropenia. This strongly argues for a cell-autonomous action of GPX4 in the erythroid system.

Vitamin E-deficiency severely aggravates erythropenia caused by GPX4-deficiency

In cell culture and in certain tissues (endothelium, T cells, hepatocytes) the phenotype of *GPX4*-deficiency can be partially or completely masked by vitamin E in vivo.[5,46-48] Vitamin E thus acts as a full or partial backup system for GPX4 in some cell types in vitro and in vivo. To exclude unintended side effects of Cre and Cre inducers or activators with vitamin E deficiency, *GPX4* was deleted prior to vitamin E deprivation. Feeding the vitamin E-depleted diet for 3 to 4 weeks to mice with *GPX4*-deficiency severely aggravated erythropenia. Despite the strong decrease in RBC as well as hemoglobin and hematocrit levels, reticulocyte counts were increased only to a small and non-significant extent (Fig.1I-M). This indicates that the anemia caused by *GPX4*-deficiency could no longer be compensated by increased production of reticulocytes when the dietary vitamin E level was reduced. In wt control mice, dietary vitamin E deprivation had no impact on red blood parameters (supplementary Fig.5). An increase of the vitamin E (i.e. α-tocopherol) concentration to the 5-fold level in the diet had no impact on erythrocyte counts, hemoglobin and hematocrit values but led to a significant decrease in reticulocyte counts (Fig.1N-R) corroborating the fact that reticulocyte counts respond more sensitively to external factors with impact on erythropoiesis than do other red blood cell parameters.

Ineffective erythropoiesis in mice with GPX4-deficient hematopoietic cells

To get deeper insight into the dynamics of *GPX4*-deficient erythropoiesis, we quantified the percentage of erythroid precursor cells in the BM and spleen by FACS analysis (Fig.2) and calculated the total numbers of erythroid precursors in these organs (Fig.3A,B). Cell suspensions of BM and spleen were stained with antibodies for CD44 or CD71 and Ter119. Erythroid precursor cells were classified into proerythroblasts based on the expression level of CD44 or CD71 and Ter119.[49,50] These analyses revealed a marked increase in extramedullary erythropoiesis in the spleen of mice with *GPX4*-deficient hematopoiesis (Fig.2H,K), and a pronounced shift towards immature precursors cells in the BM and spleen when vitamin E was additionally depleted (Fig.2F,L). The dynamic changes became more

apparent when the total numbers of erythroid precursors were calculated under the different conditions. In mice with *GPX4*-deficient hematopoietic cells the total number of proerythroblasts increased by a factor of 1.7-fold under a normal diet, and to about 4-fold when vitamin E was additionally depleted (Fig.3F). This increase was due to an increase of proerythroblasts in the spleen (Fig.3H). The number of erythroblasts in the spleen of these mice also increased significantly, and again to a much higher extent when vitamin E was depleted (Fig.3K). Under both conditions of *GPX4*-deficiency (normal versus vitamin E-depleted diet) the number of erythroblasts in the spleen increased at the expense of erythroblasts in the BM leaving the total number of erythroblasts virtually unchanged (Fig.3 I-K).

The ratio of erythrocytes to proerythroblasts illustrates the efficacy of erythropoiesis. It decreased from about 3400 in wt mice to 1340 in mice with *GPX4*-deficient hematopoiesis (Fig.3C,D). While the total number of reticulocytes increased by almost 3-fold and the ratio of reticulocytes to total proerythroblasts increased from 140 in wt mice to 240 in mice with *GPX4*-deficient hematopoiesis, RBC counts decreased to 65% (Fig.3L,M) indicating that maturation of reticulocytes to erythrocytes is defective under *GPX4*-deficiency.

Under combined *GPX4*- and vitamin E-deficiency, the ratio of erythrocytes to proerythroblasts decreased to about 250 (Fig.3E). Erythrocyte counts dropped to less than 30% (compared to wt) (Fig.3M), while the number of reticulocyte counts increased only by about 1.3 fold (Fig.3L). The only moderate and non-significant increase in reticulocyte counts is in stark contrast to the severe anemia under these conditions. The ratio of reticulocytes to total proerythroblasts decreased from 240 in mice with GPX4-deficient hematopoiesis to 45 in mice with combined *GPX4*- and vitamin E-deficiency suggesting that erythroid progenitor cells were lost during differentiation from proerythroblasts to reticulocytes, in addition to the reticulocyte maturation defect observed under these conditions. Mice with *GPX4*-deficiency in hematopoietic cells (on a normal diet) showed an increase in the size of the red pulp and the number of Ter119-positive cells (Fig.4B,E) corroborating data showing ineffective erythropoiesis. Yet, iron deposits in the red pulp stemming from physiological red blood cell turnover diminished (Fig.4B), arguing against hemolysis as the cause of anemia. Upon *GPX4*-deficiency and vitamin E depletion, the white pulp dispersed to a large extent and was intermingled with Ter119-positive erythroid cells (Fig.4C,F).

Impaired reticulocyte maturation and increased lipid peroxidation in GPX4-deficient erythroid cells and aggravation of the phenotype by vitamin E-depletion

Next, we attempted to define the maturation state of the reticulocytes in the anemic mice. To this end, peripheral blood cells were stained with CD71, Ter119, Mitotracker Deep Red, and thiazol orange. Representative examples of mice are depicted in Fig.5A-C (quantification of total numbers of mature, immature and highly immature reticulocytes in supplementary Fig.6A-F). Deletion of *GPX4* increased not only the total number of reticulocytes, but also that of each fraction: 2.1-fold of mature, 3.5-fold of immature, and 4.2-fold of highly immature reticulocytes (supplementary Fig.6D-F). The differentially higher increase in more immature reticulocytes led to a general shift towards more immature reticulocytes. Under combined *GPX4* and vitamin E deficiency, the number of highly immature reticulocytes increased 7-fold, while the total number of mature reticulocytes decreased by 20%. The failure of reticulocytes to undergo maturation was associated with an increase in lipid peroxidation of reticulocytes and erythrocytes as revealed by Bodipy 581/591-C11-staining. Lipid peroxidation was particularly pronounced in immature reticulocytes when vitamin E was additionally depleted (Fig.5D).

To further study potential subcellular alterations in response to *GPX4* loss, erythrocytes and reticulocytes of the peripheral blood were subjected to ultrastructural analysis by electron microscopy (Fig.5G-L). Reticulocytes in blood of wt mice and in blood of mice lacking *GPX4* in hematopoietic cells were characterized by remnants of ribosomes (fine granular structure) and mitochondria. An accumulation of unphagocytosed mitochondria in large vacuoles was evident when vitamin E was depleted in mice with *GPX4*-deficient hematopoiesis in vivo (white arrows in Fig.5G-L) indicating that GPX4 and vitamin E physiologically contribute to mitochondrial clearance during reticulocyte maturation.

Iron overload and oxidative stress in the liver of mice with GPX4-deficient hematopoiesis

As shown above, *GPX4*-deficiency in the hematopoietic system is characterized by ineffective erythropoiesis that is severely aggravated by additional vitamin E deprivation. Ineffective erythropoiesis is also a hallmark of β-thalassemia, and β-thalassemia is associated with iron overload that is known to sustain and to aggravate the anemia in mouse models of β-thalassemia [51]. To address whether similar mechanisms are operating in *GPX4*-deficient erythropoiesis, iron-related parameters were analyzed in the liver, spleen, and plasma of mice with *GPX4*-deficient hematopoiesis. Non-heme iron content in the liver was

significantly increased upon deletion of *GPX4* (Fig.6D). At the molecular level iron overload in the liver was confirmed by elevated levels of the iron storage protein Ferritine L (FtL) (Fig.6V). An excess of free iron triggers the formation of reactive oxygen species (ROS) and lipid peroxidation via the Fenton reaction.[3] Consistently, markers of oxidative stress such as increased lipid peroxidation products (as revealed by TBARS production) (Fig.6G) and elevated *heme oxygenase-1* mRNA and protein levels (Fig.6F,V) were detected in the liver. Combined *GPX4*- and vitamin E-deficiency further increased *heme oxygenase-1* mRNA and protein levels as well as TBARS production in the liver.

Unaltered hepcidin levels despite higher erythropoietic iron demand

Systemic iron homeostasis is maintained by the hepcidin/ferroportin regulatory system. Hepcidin regulates the amount of iron exported into systemic circulation by modulating cell surface expression of the iron exporter ferroportin on iron exporting cells. Remarkably, despite increased liver non-heme iron levels in mice with *GPX4*-deficient hematopoietic cells, hepatic *hepcidin* mRNA expression was not affected, regardless whether mice were kept on a normal or on a vitamin E-depleted diet (Fig.6H). Likewise, target genes of the iron-sensing BMP/SMAD signaling pathway in the liver (SMAD6, SMAD7, and ID1) were not significantly altered by *GPX4*- and vitamin E-deficiency (Fig.6I-K). Hepatic *ferroportin* mRNA and protein levels were increased upon *GPX4* ablation with or without vitamin E-deficiency (Fig.6E,V), a finding explained by the oxidative stress that occurs in the liver (Fig.6G). Ferroportin expression in the duodenum was unaltered (supplementary Fig.7).

We next measured iron-related plasma parameters. Plasma iron levels were not increased upon *GPX4* deletion, but were increased when *GPX4* was deleted and vitamin E simultaneously depleted (Fig.6N). Despite this, hepcidin levels in the plasma were not altered (Fig.6R). Bilirubin levels appeared to increase with ablation of *GPX4* under both conditions (± vitamin E), but the standard deviation was high so that differences became barely significant (Fig.6S-U). Consistent with elevated liver iron levels, plasma ferritin was highly increased under combined *GPX4*- and vitamin E-deficiency (Fig.6O).

In mouse models with β-thalassemia plasma erythropoietin (EPO) levels are increased. EPO stimulates the expression of the blood hormone erythroferrone (ERFE) in erythroid precursor cells, which then down regulates hepcidin levels. Similarly, EPO and ERFE levels appeared to be increased in mice with *GPX4*-deficient hematopoiesis, but only EPO levels reached significance. Under combined *GPX4*- and vitamin E-deficiency plasma EPO and ERFE

levels increased to very high and highly significant levels (Fig.6P,Q), apparently mirroring the severity of erythropenia under combined *GPX4*- and vitamin E-deficiency.[52] Taken together, the defect in reticulocyte maturation by loss of the *GPX4* gene causes ineffective erythropoiesis with simultaneous iron overload in the liver and iron-deficiency in the hematopoietic system and this phenotype is to a large part masked by vitamin E in the normal diet.

DISCUSSION

Based on biochemical studies Schewe et al. reported in 1975 that mitochondrial clearance during reticulocyte maturation is initiated by enzymatic lipid peroxidation.[20] These authors purified the enzyme 15-lipoxygenase from rabbit reticulocytes and showed that it oxidizes polyunsaturated fatty acids in mitochondrial membranes as initiating event in the disposal of mitochondria. Even though the work has been confirmed and extended by others,[24,25] these studies fell into oblivion due to the fact that erythropoiesis including erythrocyte and reticulocyte counts appeared to be normal in mice lacking 12/15-lipoxygenase.[26]

Since a few years the work of the Rapoport group is, however, regaining attention due to several important novel findings: (i) GPX4 was shown to be an antagonist of a novel 12/15-lipoxygenase-induced, non-apoptotic cell death pathway in murine fibroblasts,[5] (ii) this mode of cell death initiated by ablation of *GPX4* has been shown to be driven by iron-induced lipid peroxidation and is now known as ferroptosis,[2,31,47,53] (iii) distinct phospholipid hydroperoxide species have been identified that act as death signals and inducers of ferroptosis in various cell types,[54] (iv) vitamin E synergizes with GPX4 in antagonizing the action of lipid hydroxyperoxides in vitro and in vivo,[46-48,55] (v) 12/15-lipoxygenase and its hydroxylated oxidation products are involved in the regulation of autophagy in murine macrophages,[19] (vi) autophagy is inhibited by oxidation of enzymes like Atg3 and Atg7 that catalyze Atg8/LC3 lipidation,[56] (vii) lipoxygenases are not necessarily the decisive source of lipid hydroperoxides, they may rather sensitize cells to iron-mediated non-enzymatic autoxidation.[29]

It was the aim of our study to identify a missing link between membrane lipid oxidation and reticulocyte maturation by genetic means. Based on the finding that GPX4 is unique in antagonizing lipid membrane hydroperoxides and stabilizing the hydroxylated oxidation products,[6,8] we hypothesized that deletion of *GPX4* in hematopoietic cells would perturb mitophagy and thus reticulocyte maturation.

The role of GPX4 in hematopoietic cells had already been studied by Canli et al. using *GPX4*$^{fl/fl}$*;Mx1-Cre* mice.[55] These authors primarily focused, however, on the mode of cell death in hematopoietic precursor cells and not on a comprehensive view on *GPX4*-deficient erythropoiesis at a quantitative level.

As an inducible knockout model for *GPX4* exclusively in hematopoietic cells, we have reconstituted lethally irradiated wt mice with *GPX4*$^{fl/fl}$*;Cre-ERT2* or *GPX4*$^{wt/wt}$*;CreERT2* BM cells. We now show that activation of Cre by feeding a tamoxifen-containing diet induces an aplastic anemia affecting red as well as white blood cells not only in mice reconstituted with *GPX4*-deficient, but also in control mice with *GPX4*$^{wt/wt}$*;CreERT2* BM cells thus confirming the acute toxic effect of Cre activation on the hematopoietic system described by Higashi et al.[33] There is, however, a clear difference between mice harboring or lacking the *GPX4* gene in hematopoietic cells: mice reconstituted with *GPX4*$^{wt/wt}$*;CreERT2* BM cells recovered within 3 to 6 weeks whereas mice reconstituted with cells lacking the *GPX4* gene failed to fully recover and remained partially anemic. The erythropenic phenotype could be stably transmitted into lethally irradiated wt mice by two consecutive rounds of transplantation. It is noteworthy that Cre activation by tamoxifen and *GPX4* ablation cause different types of anemia. Cre activation leads to an aplastic anemia with cessation of red blood cell (supplementary Fig.1F) and white blood cell formation (supplementary Fig.1L-P), whereas ablation of *GPX4* in the hematopoietic system causes ineffective erythropoiesis with increased formation of reticulocytes (Fig.1H). As recovery from anemia as well as from hematopoietic reconstitution is driven by stress erythropoiesis,[43] stress erythropoiesis is perturbed by *GPX4*-deficiency in hematopoietic cells. Depletion of vitamin E in the diet strongly aggravated the anemic phenotype. To exclude unintended side effects of vitamin E depletion with the well-known toxicity of Cre and Cre inducers and activators, the *GPX4* gene was deleted prior to vitamin E depletion. The dynamics of erythropoiesis under the various conditions including the maturation state of reticulocytes was assessed by FACS staining of proerythroblasts and erythroblasts in the BM and spleen and of reticulocytes in the peripheral blood. A more comprehensive picture emerged (i) by calculating the total number of proerythroblasts and erythroblasts in the BM and spleen, (ii) by extrapolating to the total number of reticulocytes and erythrocytes per mouse, and (iii) by quantifying the fraction of mature, immature and highly immature reticulocytes.

In mice with *GPX4*-deficient hematopoiesis the total number of proerythroblasts was increased, mainly due to an increase in extramedullary erythropoiesis. Total numbers of mature, immature as well as highly immature reticulocytes were also increased. The differentially higher increase in immature and highly immature reticulocytes led to a shift

towards immature reticulocytes. This indicates that under hematopoietic *GPX4*-deficiency the rate of reticulocyte production exceeded the rate of reticulocyte maturation, a disequilibrium that resulted in ineffective erythropoiesis.

Under combined *GPX4*- and vitamin E-deficiency the number of proerythroblasts in the spleen was further strongly increased. Within the reticulocyte fraction, there was a pronounced shift towards highly immature reticulocytes. Yet, production of reticulocytes did not keep up with the production of proerythroblasts as total reticulocyte counts were not significantly higher than in wt mice. This suggests that, in addition to the severe reticulocyte maturation defect, erythroid progenitor cells were lost during differentiation from the proerythroblast to the reticulocyte stage. Highest levels of lipid peroxidation, as assessed by C11-Bodipy(581/591)-staining, were observed in immature reticulocytes under combined *GPX4*- and vitamin E-deficiency which correlates with the severity of the phenotype. Ultrastructural analysis revealed remnants of mitochondria and ribosomes in reticulocytes of wt mice and mice with *GPX4*-deficient hematopoiesis, and a pronounced accumulation of large vacuoles containing unphagocytosed mitochondria, when dietary vitamin E was lowered. The data support the model that mitophagy is triggered by lipid oxidation that is kept in check by GPX4. Hence, loss of *GPX4*, especially under vitamin E-restricted conditions, leads to uncontrolled lipid peroxidation and as a consequence, to severely perturbed mitophagy (Fig.7).

The anemia caused by hematopoietic *GPX4*-deficiency shares a number of features with β-thalassemia, for which the term ineffective erythropoiesis has been coined: decreased RBC, elevated reticulocyte counts, overactive extramedullary erythropoiesis, elevated erythroid progenitors, absence of hemolysis, and systemic iron overload linked to severe iron demand for the erythroid system.[51] This prompted us to study iron metabolism in mice with *GPX4*-deficient hematopoiesis. Hematopoietic *GPX4*–deficiency caused liver iron overload and oxidative stress, elevated plasma ferritin and iron levels, parameters aggravated by vitamin E depletion. Despite signs of iron overload in the liver and plasma, there was continuous demand for iron in the erythroid system. As a consequence of the anemia, plasma EPO and ERFE levels were elevated. Likewise, *Erfe* splenic mRNA expression was increased, particularly when *GPX4* deletion and vitamin E-deficiency were combined. Since ERFE mirrors the erythropoietic activity[52,57] and there is virtually no background of extramedullary erythropoiesis in the spleen of wt mice under steady state conditions, spleen *Erfe* mRNA emerged as the most sensitive parameter of iron demand.

Despite the dramatic increase in ERFE production in mice with combined *GPX4*- and vitamin E-deficiency, hepcidin expression in the liver plasma was unchanged. This is reminiscent to what has been observed in β-thalassemic Th3/+ mice older than 6 weeks.[57] Suppression of *hepcidin* expression is only seen when the mice are young and still loading their livers with iron. Once enough iron is loaded, hepcidin begins to rise, driven by hepatic iron stores, despite high erythroferrone, so that older mice have high liver iron but normal hepcidin that slows down further iron loading. Thus, hypoxia and elevated iron demand for erythropoiesis decrease *hepcidin* expression, whereas high plasma and hepatic iron levels counteract the response to ERFE in the liver. An alternative explanation is that a yet-unrecognized factor induced in response to oxidative stress or a direct oxidative modification of ERFE counteracts the action of ERFE on *hepcidin* expression.

The pronounced similarity between anemia caused by hematopoietic *GPX4*-deficiency and β-thalassemia raises the question whether underlying pathogenic principles are shared between both conditions. A common denominator is by no doubt the involvement of oxygen radicals. In case of *GPX4*-deficiency, they arise from increased lipid peroxidation, in case of β-thalassemia from inappropriate folding of globin chains and hemoglobin assembly. This liberates oxygen, heme and iron thus favoring the production of oxygen radicals through non-enzymatic autoxidation.[27,28,58] There is ample evidence in the literature that increased lipid peroxidation in red blood cells and decreased lipid-soluble antioxidant levels in the plasma as well as in erythrocytes are consistent features of β-thalassemia.[59-63] Administration of vitamin E normalized the plasma oxidant/antioxidant balance and vitamin E content of erythrocytes, yet, the clinical benefit of vitamin E administration remained limited due to the persistence of iron-overload in affected patients[62-65]. Taken together, perturbed reticulocyte maturation through uncontrolled lipid peroxidation may be the underlying cause of ineffective erythropoiesis in both conditions.

It still remains unclear to which extent lipoxygenase-mediated enzymatic and/or non-enzymatic mechanisms contribute to lipid peroxidation in the anemia described here. Lipoxygenases lower the threshold for non-enzymatic autoxidation[29] and may be required for initiating lipid oxidation in mitochondrial membranes. In the absence of 12/15-lipoxygenase other lipoxygenases may functionally compensate for the loss of the missing enzyme. A scenario of non-enzymatic lipid peroxidation is, however, also conceivable. Once lipid peroxidation is triggered, the process may be self-sustaining due to the high concentration of iron, heme compounds and oxygen rendering enzymatic lipid peroxidation dispensable.

Another critical determinant of physiological reticulocyte maturation is the cholesterol concentration in the reticulocyte membrane as well as in the plasma. Holm et al. have shown in an elegant study that mice lacking apolipoprotein E and high-density lipid protein receptor I (SR-BI) are unable to expel autophagocytosed organelles and accumulate autophagolysosomes in their reticulocytes.[66] These mice lack mature erythrocytes and their gas transport relies exclusively on reticulocytes. Remarkably, the block in terminal reticulocyte maturation is cell-non-autonomous in these mice and reversible: transfusion of these reticulocytes into wt mice or hematopoietic reconstitution of lethally irradiated wt mice with apoliporotein E- and SR-BI-deficient BM cells completely normalized reticulocyte maturation. The phenotype could also be reversed through sequestration of free cholesterol: administration of cyclodextrin led to immediate expulsion of stored autophagolysosomes in vivo and in vitro and normalized the phenotype. At the contrary to the apolipoprotein E- and SR-BI-model of Holm et al., we are dealing in our model with a cell-autonomous effect of *GPX4*-deficiency to which cell-nonautonomous factors like the plasma concentration of vitamin E also contribute to a significant extent. In both conditions, the precise molecular underpinnings underlying the defects in reticulocyte maturation await to be elucidated.

ACKNOWLEDGEMENTS

MUM acknowledges funding from the Deutsche Forschungsgemeinschaft (SFB1036, SFB1118); S.A. is supported by the European Hematology Association (Advanced Research fellowship). Support by the German Federal Ministry of Education and Research Infrafrontier grant 01KX1012 for German Mouse Clinic (GMC) infrastructure (to MHA). We thank Prof. Anton Berns, the Netherland Cancer Institute, Amsterdam, for providing *Rosa26;CreERT2* mice. MC and GWB thank Matilde Maiorino and Fulvio Ursini for many helpful discussions. We are most grateful to Martina Mötscher, Jasmin Teutsch and Michael Hagemann for breeding the mice.

AUTHOR CONTRIBUTION

Transplantation experiments were performed by NV. Blood parameters of GPX4fl/fl;CreERT2 mice and controls were analyzed by LH, MS, CL, CKR, BR, and GWB using the Sysmex XT-2000iV apparatus which could be purchased through a grant to MHA. Blood parameters, bone marrow blood island macrophages and spleen red pulp macrophages of GPX4fl/fl;LysM-Cre and control mice were analyzed by KO and MK. Tissue specimens were prepared by PH, LH, MS, CL, CKR, and GWB. PCR, quantitative RT-PCR and western blot analyses were performed by SA. FACS analysis of blood, BM, and spleen cells was done by PH, TS, JM, CL, and CKR. Histology was performed and evaluated by SA, DJ and FN. Ultrastructural analysis was performed by MA and AW. Parameters of iron metabolism were determined by SA, ARS, KM and TG (ERFE). NV, CB, SA, MUM, TS, MC, and GWB designed the concept and evaluated data. Figures were prepared by SA, NV, MK, MC, and GWB. GWB wrote the manuscript with significant contributions from SA, NV, MC, TG, MK, and MUM.

CONFLICT OF INTEREST DISCLOSURE

There is no conflict of interest.

REFERENCES

1. Ursini F, Maiorino M, Valente M, Ferri L, Gregolin C. Purification from pig liver of a protein which protects liposomes and biomembranes from peroxidative degradation and exhibits glutathione peroxidase activity on phosphatidylcholine hydroperoxides. Biochim Biophys Acta. 1982;710(2):197-211.
2. Maiorino M, Conrad M, Ursini F. GPx4, Lipid Peroxidation, and Cell Death: Discoveries, Rediscoveries, and Open Issues. Antioxid Redox Signal. 2018;29(1):61-74.
3. Hentze MW, Muckenthaler MU, Andrews NC. Balancing acts: molecular control of mammalian iron metabolism. Cell. 2004;117(3):285-297.
4. Bordet JC, Guichardant M, Lagarde M. Hydroperoxides produced by n-6 lipoxygenation of arachidonic and linoleic acids potentiate synthesis of prostacyclin related compounds. Biochim Biophys Acta. 1988;958(3):460-468.
5. Seiler A, Schneider M, Forster H, et al. Glutathione peroxidase 4 senses and translates oxidative stress into 12/15-lipoxygenase dependent- and AIF-mediated cell death. Cell Metab. 2008;8(3):237-248.
6. Thomas JP, Maiorino M, Ursini F, Girotti AW. Protective action of phospholipid hydroperoxide glutathione peroxidase against membrane-damaging lipid peroxidation. In situ reduction of phospholipid and cholesterol hydroperoxides. J Biol Chem. 1990;265(1):454-461.
7. Weitzel F, Wendel A. Selenoenzymes regulate the activity of leukocyte 5-lipoxygenase via the peroxide tone. J Biol Chem. 1993;268(9):6288-6292.
8. Schnurr K, Belkner J, Ursini F, Schewe T, Kuhn H. The selenoenzyme phospholipid hydroperoxide glutathione peroxidase controls the activity of the 15-lipoxygenase with complex substrates and preserves the specificity of the oxygenation products. J Biol Chem. 1996;271(9):4653-4658.
9. Kuhn H, Borchert A. Regulation of enzymatic lipid peroxidation: the interplay of peroxidizing and peroxide reducing enzymes. Free Radic Biol Med. 2002;33(2):154-172.
10. Kryukov GV, Castellano S, Novoselov SV, et al. Characterization of mammalian selenoproteomes. Science. 2003;300(5624):1439-1443.
11. Burk RF, Hill KE. Regulation of Selenium Metabolism and Transport. Annu Rev Nutr. 2015;35:109-134.
12. Ingold I, Berndt C, Schmitt S, et al. Selenium Utilization by GPX4 Is Required to Prevent Hydroperoxide-Induced Ferroptosis. Cell. 2018;172(3):409-422.
13. Liao C, Hardison RC, Kennett MJ, Carlson BA, Paulson RF, Prabhu KS. Selenoproteins regulate stress erythroid progenitors and spleen microenvironment during stress erythropoiesis. Blood. 2018;131(23):2568-2580.
14. Kaushal N, Hegde S, Lumadue J, Paulson RF, Prabhu KS. The regulation of erythropoiesis by selenium in mice. Antioxid Redox Signal. 2011;14(8):1403-1412.
15. Schweers RL, Zhang J, Randall MS, et al. NIX is required for programmed mitochondrial clearance during reticulocyte maturation. Proc Natl Acad Sci U S A. 2007;104(49):19500-19505.
16. Sandoval H, Thiagarajan P, Dasgupta SK, et al. Essential role for Nix in autophagic maturation of erythroid cells. Nature. 2008;454(7201):232-235.
17. Chu CT, Ji J, Dagda RK, et al. Cardiolipin externalization to the outer mitochondrial membrane acts as an elimination signal for mitophagy in neuronal cells. Nat Cell Biol. 2013;15(10):1197-1205.
18. Kagan VE, Tyurina YY, Tyurin VA, et al. Cardiolipin signaling mechanisms: collapse of asymmetry and oxidation. Antioxid Redox Signal. 2015;22(18):1667-1680.
19. Morgan AH, Hammond VJ, Sakoh-Nakatogawa M, et al. A novel role for 12/15-lipoxygenase in regulating autophagy. Redox Biol. 2015;4:40-47.
20. Schewe T, Halangk W, Hiebsch C, Rapoport SM. A lipoxygenase in rabbit reticulocytes which attacks phospholipids and intact mitochondria. FEBS Lett. 1975;60(1):149-152.

21. Rapoport SM, Schewe T, Wiesner R, et al. The lipoxygenase of reticulocytes. Purification, characterization and biological dynamics of the lipoxygenase; its identity with the respiratory inhibitors of the reticulocyte. Eur J Biochem. 1979;96(3):545-561.
22. Rapoport SM, Schewe T. The maturational breakdown of mitochondria in reticulocytes. Biochim Biophys Acta. 1986;864(3-4):471-495.
23. Kuhn H, Brash AR. Occurrence of lipoxygenase products in membranes of rabbit reticulocytes. Evidence for a role of the reticulocyte lipoxygenase in the maturation of red cells. J Biol Chem. 1990;265(3):1454-1458.
24. van Leyen K, Duvoisin RM, Engelhardt H, Wiedmann M. A function for lipoxygenase in programmed organelle degradation. Nature. 1998;395(6700):392-395.
25. Grullich C, Duvoisin RM, Wiedmann M, van Leyen K. Inhibition of 15-lipoxygenase leads to delayed organelle degradation in the reticulocyte. FEBS Lett. 2001;489(1):51-54.
26. Sun D, Funk CD. Disruption of 12/15-lipoxygenase expression in peritoneal macrophages. Enhanced utilization of the 5-lipoxygenase pathway and diminished oxidation of low density lipoprotein. J Biol Chem. 1996;271(39):24055-24062.
27. Szebeni J, Winterbourn CC, Carrell RW. Oxidative interactions between haemoglobin and membrane lipid. A liposome model. Biochem J. 1984;220(3):685-692.
28. NaveenKumar SK, SharathBabu BN, Hemshekhar M, Kemparaju K, Girish KS, Mugesh G. The Role of Reactive Oxygen Species and Ferroptosis in Heme-Mediated Activation of Human Platelets. ACS Chem Biol. 2018;13(8):1996-2002.
29. Shah R, Shchepinov MS, Pratt DA. Resolving the Role of Lipoxygenases in the Initiation and Execution of Ferroptosis. ACS Cent Sci. 2018;4(3):387-396.
30. Yant LJ, Ran Q, Rao L, et al. The selenoprotein GPX4 is essential for mouse development and protects from radiation and oxidative damage insults. Free Radic Biol Med. 2003;34(4):496-502.
31. Friedmann Angeli JP, Schneider M, Proneth B, et al. Inactivation of the ferroptosis regulator Gpx4 triggers acute renal failure in mice. Nat Cell Biol. 2014;16(12):1180-1191.
32. Hameyer D, Loonstra A, Eshkind L, et al. Toxicity of ligand-dependent Cre recombinases and generation of a conditional Cre deleter mouse allowing mosaic recombination in peripheral tissues. Physiol Genomics. 2007;31(1):32-41.
33. Higashi AY, Ikawa T, Muramatsu M, et al. Direct hematological toxicity and illegitimate chromosomal recombination caused by the systemic activation of CreERT2. J Immunol. 2009;182(9):5633-5640.
34. Loonstra A, Vooijs M, Beverloo HB, et al. Growth inhibition and DNA damage induced by Cre recombinase in mammalian cells. Proc Natl Acad Sci U S A. 2001;98(16):9209-9214.
35. Zhu J, Nguyen MT, Nakamura E, Yang J, Mackem S. Cre-mediated recombination can induce apoptosis in vivo by activating the p53 DNA damage-induced pathway. Genesis. 2012;50(2):102-111.
36. Janbandhu VC, Moik D, Fassler R. Cre recombinase induces DNA damage and tetraploidy in the absence of loxP sites. Cell Cycle. 2014;13(3):462-470.
37. Pepin G, Ferrand J, Honing K, et al. Cre-dependent DNA recombination activates a STING-dependent innate immune response. Nucleic Acids Res. 2016;44(11):5356-5364.
38. Huh WJ, Khurana SS, Geahlen JH, Kohli K, Waller RA, Mills JC. Tamoxifen induces rapid, reversible atrophy, and metaplasia in mouse stomach. Gastroenterology. 2012;142(1):21-24.
39. Velasco-Hernandez T, Sawen P, Bryder D, Cammenga J. Potential Pitfalls of the Mx1-Cre System: Implications for Experimental Modeling of Normal and Malignant Hematopoiesis. Stem Cell Reports. 2016;7(1):11-18.
40. Kiermayer C, Conrad M, Schneider M, Schmidt J, Brielmeier M. Optimization of spatiotemporal gene inactivation in mouse heart by oral application of tamoxifen citrate. Genesis. 2007;45(1):11-16.

41. Rathkolb B, Fuchs H, Gailus-Durner V, Aigner B, Wolf E, Hrabe de Angelis M. Blood Collection from Mice and Hematological Analyses on Mouse Blood. Curr Protoc Mouse Biol. 2013;3(2):101-119.
42. Lenox LE, Perry JM, Paulson RF. BMP4 and Madh5 regulate the erythroid response to acute anemia. Blood. 2005;105(7):2741-2748.
43. Harandi OF, Hedge S, Wu DC, McKeone D, Paulson RF. Murine erythroid short-term radioprotection requires a BMP4-dependent, self-renewing population of stress erythroid progenitors. J Clin Invest. 2010;120(12):4507-4519.
44. Chasis JA, Mohandas N. Erythroblastic islands: niches for erythropoiesis. Blood. 2008;112(3):470-478.
45. Clausen BE, Burkhardt C, Reith W, Renkawitz R, Forster I. Conditional gene targeting in macrophages and granulocytes using LysMcre mice. Transgenic Res. 1999;8(4):265-277.
46. Wortmann M, Schneider M, Pircher J, et al. Combined deficiency in glutathione peroxidase 4 and vitamin E causes multiorgan thrombus formation and early death in mice. Circ Res. 2013;113(4):408-417.
47. Matsushita M, Freigang S, Schneider C, Conrad M, Bornkamm GW, Kopf M. T cell lipid peroxidation induces ferroptosis and prevents immunity to infection. J Exp Med. 2015;212(4):555-568.
48. Carlson BA, Tobe R, Yefremova E, et al. Glutathione peroxidase 4 and vitamin E cooperatively prevent hepatocellular degeneration. Redox Biol. 2016;9:22-31.
49. Chen K, Liu J, Heck S, et al. Resolving the distinct stages in erythroid differentiation based on dynamic changes in membrane protein expression during erythropoiesis. Proc Natl Acad Sci U S A. 2009;106(41):17413-17418.
50. Marsee DK, Pinkus GS, Yu H. CD71 (transferrin receptor): an effective marker for erythroid precursors in bone marrow biopsy specimens. Am J Clin Pathol. 2010;134(3):429-435.
51. Rivella S. Ineffective erythropoiesis and thalassemias. Curr Opin Hematol. 2009;16(3):187-194.
52. Kautz L, Jung G, Valore EV, Rivella S, Nemeth E, Ganz T. Identification of erythroferrone as an erythroid regulator of iron metabolism. Nat Genet. 2014;46(7):678-684.
53. Yang WS, SriRamaratnam R, Welsch ME, et al. Regulation of ferroptotic cancer cell death by GPX4. Cell. 2014;156(1-2):317-331.
54. Kagan VE, Mao G, Qu F, et al. Oxidized arachidonic and adrenic PEs navigate cells to ferroptosis. Nat Chem Biol. 2017;13(1):81-90.
55. Canli O, Alankus YB, Grootjans S, et al. Glutathione peroxidase 4 prevents necroptosis in mouse erythroid precursors. Blood. 2016;127(1):139-148.
56. Frudd K, Burgoyne T, Burgoyne JR. Oxidation of Atg3 and Atg7 mediates inhibition of autophagy. Nat Commun. 2018;9(1):95.
57. Kautz L, Jung G, Du X, et al. Erythroferrone contributes to hepcidin suppression and iron overload in a mouse model of beta-thalassemia. Blood. 2015;126(17):2031-2037.
58. Tappel AL. Unsaturated lipide oxidation catalyzed by hematin compounds. J Biol Chem. 1955;217(2):721-733.
59. Rachmilewitz EA, Shohet SB, Lubin BH. Lipid membrane peroxidation in beta-thalassemia major. Blood. 1976;47(3):495-505.
60. Rachmilewitz EA, Shifter A, Kahane I. Vitamin E deficiency in beta-thalassemia major: changes in hematological and biochemical parameters after a therapeutic trial with alpha-tocopherol. Am J Clin Nutr. 1979;32(9):1850-1858.
61. Rachmilewitz EA, Kornberg A, Acker M. Vitamin E deficiency due to increased consumption in beta-thalassemia and in Gaucher's disease. Ann N Y Acad Sci. 1982;393:336-347.
62. Fibach E, Rachmilewitz EA. The role of antioxidants and iron chelators in the treatment of oxidative stress in thalassemia. Ann N Y Acad Sci. 2010;1202:10-16.

63. Livrea MA, Tesoriere L, Pintaudi AM, et al. Oxidative stress and antioxidant status in beta-thalassemia major: iron overload and depletion of lipid-soluble antioxidants. Blood. 1996;88(9):3608-3614.
64. Giardini O, Cantani A, Donfrancesco A, et al. Biochemical and clinical effects of vitamin E administration in homozygous beta-thalassemia. Acta Vitaminol Enzymol. 1985;7(1-2):55-60.
65. Tesoriere L, D'Arpa D, Butera D, et al. Oral supplements of vitamin E improve measures of oxidative stress in plasma and reduce oxidative damage to LDL and erythrocytes in beta-thalassemia intermedia patients. Free Radic Res. 2001;34(5):529-540.
66. Holm TM, Braun A, Trigatti BL, et al. Failure of red blood cell maturation in mice with defects in the high-density lipoprotein receptor SR-BI. Blood. 2002;99(5):1817-1824.

FIGURE LEGENDS

Figure 1:

A-H) GPX4 is required for stress erythropoiesis in the recovery phase of anemia. Deletion of GPX4 in the bone marrow was monitored by PCR using two primers pairs. One detects the deleted allele (509 bp), the other discriminates between the floxed and wt allele. Absence of the floxed allele indicates that deletion was complete. Presence of the wt band indicates that bone marrow cells contain a small proportion of cells of non-hematopoietic origin (A). Quantification of GPX4 mRNA in the bone marrow by quantitative RT-PCR (B). Detection of GPX4 protein by western blot analysis (C). Temporal scheme of bone marrow transplantation (BMT), tamoxifen treatment (TAM) and determination of RBC parameters (D). Lethally irradiated mice were reconstituted with 10^6 BM cells of *GPX4*$^{wt/wt}$*;Cre-ERT2* (designated wt, black columns, n=10) and *GPX4*$^{fl/fl}$*;Cre-ERT2* mice (designated k.o., grey columns, n=19). Mice were fed a tamoxifen citrate containing diet for three weeks. Blood was drawn before (left columns, - TAM), at the last day of (0), and 3, 6, and 9 weeks after tamoxifen administration (+TAM), and erythrocyte counts (E), hemoglobin (F), hematocrit (G), and reticulocyte counts were determined (H).

I-M) Vitamin E depletion in the diet severely aggravates the anemia caused by *GPX4*-deficiency in hematopoietic cells. Temporal scheme of BMT, tamoxifen administration, vitamin E depletion and determination of red blood parameters (I). Lethally irradiated mice were reconstituted with BM cells of *GPX4*$^{wt/wt}$*;Cre-ERT2* (designated wt, black columns) and *GPX4*$^{fl/fl}$*;Cre-ERT2* mice (designated k.o., grey and white columns). After tamoxifen administration for 3 weeks, mice were allowed to recover for 12 weeks before the vitamin E-depleted diet was started (- vitE, n=7 for wt, n=7 for k.o.) or the normal diet continued (+ vitE, n=3 for wt, n=7 for k.o.). Blood was drawn before vitamin E depletion (time point 9 weeks in Fig.1D-H), and 26 (black and grey columns) and 54 days (white columns), n=3) after starting the vitamin E-depleted diet for the determination of erythrocyte counts (J), hemoglobin (K), hematocrit levels (L), and reticulocyte counts (M). Red blood parameters of blood taken 54 days after starting the vitamin E-depleted diet were unaltered as compared to the earlier time point.

N-R) Administration of a vitamin E-enriched diet. Temporal scheme of feeding the mice a vitamin E-enriched diet (N). A 5-fold increase of α-tocopherol in the diet reduced the degree of reticulocytosis (R) but had not impact on erythrocyte counts (O), hemoglobin (P) and hematocrit (Q).

S-W) White blood counts and red blood parameters and in GPXfl/fl;LysM-Cre and control mice. There is no difference in white blood cell counts (S), erythrocytes (T), hemoglobin (U), hematocrit (V), and reticulocyte counts (W) between GPXfl/fl;LysM-Cre and control mice.

Figure 2:

Relative increase in immature erythroid precursor cells in the bone marrow and spleen of mice with *GPX4*-deficiency in the hematopoetic system. Representative FACS staining of bone marrow (A-F) and spleen cells (G-L) with CD44-PE-Cy7 and Ter119-PE (A-C) as well as with CD71-PE-Cy7 and Ter119-PE antibodies (D-F, J-L). The gate set by forward sideward scatter (FSC) and lineage marker-negative cells (G-I) illustrates the increase in extramedullary erythropoiesis in the spleen of mice with GPX4-deficient hematopoietic cells kept on a normal (H) or on a vitamin E-depleted diet (I) as compared to *GPX4* wt mice kept on a normal diet (G). The shift towards immature erythroid precursor cells is strongly increased under combined *GPX4*- and vitamin E-deficiency (C, F, L).

Figure 3:

Ineffective erythropoiesis in mice with *GPX4*-deficiency in the hematopoietic system and severe aggravation by dietary vitamin E deficiency. Total numbers of bone marrow cells collected from two femura and two tibiae (A) and spleen weights (B) of wt mice (n=8) and of mice with *GPX4*-deficient hematopoiesis maintained either on a normal (n=8) or a vitamin E-depleted diet (n=9). The total numbers of proerythroblasts and erythroblasts in the bone marrow and spleen, and of reticulocytes and erythrocytes in the blood were assessed as described in the supplementary information. Comparative quantification of the total numbers of proerythroblasts (F-H, n=8 for each condition), of erythroblasts (I-K, n=8 for each condition), reticulocytes (L) and erythrocytes (M, both n=42 wt; n=23 k.o., normal diet; n=16 k.o. minus vitE). Proerythroblasts in the bone marrow and spleen were quantified separately in G and H, and erythroblasts in J and K, respectively. The significance was calculated by the Mann-Whitney test. The erythropenia caused by *GPX4*-deficiency in hematopoietic cells is compensated to a large extent by increased extramedullary erythropoiesis and strongly elevated reticulocyte counts. Under combined *GPX4*- and vitamin E-deficiency, the number or erythrocytes is strongly decreased, but the number of reticulocytes is not significantly higher than in wt mice. This points to a loss of erythroid progenitor cells at the

proerythroblast and/or erythroblast stage in addition to the reticulocyte maturation defect under these conditions.

Figure 4:

Extramedullary hematopoiesis in lethally irradiated wt mice reconstituted with *GPX4*-deficient bone marrow cells. Histological sections of the spleen (A-F) of *GPX4* wt mice kept on a normal diet (A,D), and of mice with *GPX4*-deficient hematopoiesis maintained either on a normal (B,E) or on a vitamin E-depleted diet (C,F), stained with Perls´ blue stain (A-C) or by immunohistochemistry with anti-Ter119 antibody (D-F). The splenic red pulp is increased in mice with *GPX4*-deficient hematopoiesis (B,E) and the white pulp is almost completely dissipated when vitamin E is additionally depleted (C,F). Iron deposits derived from erythrocyte turnover are clearly visible in the red pulp of wt mice kept on a normal diet (A), but are only faintly visible in the periphery of follicles in the white pulp of mice with *GPX4*-deficient hematopoiesis (B,C). Iron deposits are decreased rather than increased in the spleen of severely anemic mice arguing against increased hemolysis as the cause of anemia.

Figure 5:

A-C) *GPX4*-deficiency in hematopoietic cells causes a reticulocyte maturation defect that is to a large extent compensated by vitamin E in vivo. Representative FACS stainings of peripheral blood cells of *GPX4* wt mice kept on a normal diet (A), and of mice with *GPX4*-deficient hematopoiesis maintained either on a normal (B) or on a vitamin E-depleted diet (C), stained with Mitotracker Deep Red (MTDR), thiazol orange (TO), and CD71-PE-Cy7 and Ter119-PE antibodies. The experiment is described and quantitatively evaluated in supplementary Fig.5. Ter119-positive cells were gated and plotted as shown in A-C. Immature reticulocytes ($CD71^{high}$) are shown in green, mature reticulocytes ($CD71^{low}$) in blue and erythrocytes ($CD71^{neg}/Ter119^{+}$) in purple. $CD71^{high}$ cells were subdivided into immature and highly immature reticulocytes based on MTDR and TO staining. Under combined *GPX4*- and vitamin E-deficiency the fraction of highly immature reticulocytes was strongly increased (C).

D-F) Lipid peroxidation is increased in *GPX4*-deficient reticulocytes and erythrocytes. Peripheral blood cells of the mice shown in A-C mice were stained with anti-CD71-PE-Cy7-

and anti-Ter119-APC-Cy7-antibodies and with 2µM C11-Bodipy(581/591). Ter119-positive cells were gated and the increase in % green fluorescence-positive cells was measured in $CD71^{high}$ cells (immature reticulocytes, D), in $CD71^{low}$ cells (mature reticulocytes, E) and in $CD71^{neg}$ cells (erythrocytes, F) upon excitation at 488 nm. Wild type, normal diet, (n=2); k.o., normal diet (n=2); k.o., minus vitamin E (n=3). The significance was calculated using an unpaired T-Test. Note the high degree of lipid peroxidation in *GPX4*-deficient immature reticulocytes upon feeding a vitamin E-depleted diet.

G-L) Ultrastructural analysis of red blood cells from the mice shown in A-C. Remnants of mitochondria (Mi) are marked by white arrows. Under *GPX4* deficiency (H and K), and more so under combined *GPX4*- and vitamin E-deficiency (I and L) large unphagocytosed vesicles containing mitochondria accumulated in reticulocytes (R). Blood pellets were processed for transmission electron microscopy as described in the supplementary information.

Figure 6:

Iron overload in the liver and simultaneous iron demand for erythropoiesis in mice with a *GPX4*- deficient hematopoietic system. In the liver of mice with GPX4-proficient and GPX4-deficient hematopoiesis only the wt allele of *GPX4* is detected (A), and the same levels of *GPX4* mRNA (B) and protein (C) are expressed. Parameters of iron metabolism in the liver (D-K,V): Non-heme hepatic iron (D), *ferroportin* mRNA (E), *heme oxygenase-1* mRNA (F), thiobarbituric acid reactive substances (TBARS)(G), *hepcidin* mRNA (H), *Smad6* mRNA (I), *Smad7* mRNA (J), and *ID1* mRNA (K). The proteins ferroportin (Fpn), heme oxygenase (HO-1), and ferritine light chain (FtL) are expressed at higher level in mice with a *GPX4*-deficient hematopoietic system (V). Parameters of splenic and peripheral iron metabolism: non-heme splenic iron (L), *splenic Erfe* mRNA (M), plasma iron (N), plasma ferritine (O), plasma EPO (P), plasma ERFE (Q), plasma hepcidin (R), plasma bilirubin total (S), plasma bilirubin direct (T), plasma bilirubin indirect (U). Increased hepatic non-heme iron and TBARS as well as elevated ferroportin and heme oxygenase-1 expression point to hepatic iron overload, whereas highly increased EPO and ERFE levels in the plasma and elevated *Erfe* mRNA expression levels are strong indicators of severe iron demand in the erythropoietic system. Note that hepcidin expression is not down regulated despite the strong erythropoietic iron demand. For HO-1/actin ratio in the liver and duodenal ferroportin expression, see supplementary Fig.7A,B.

Figure 7:

Proposed model for the role of 12/15-lipoxygenase, GPX4 and vitamin E during reticulocyte maturation.

Figure 1

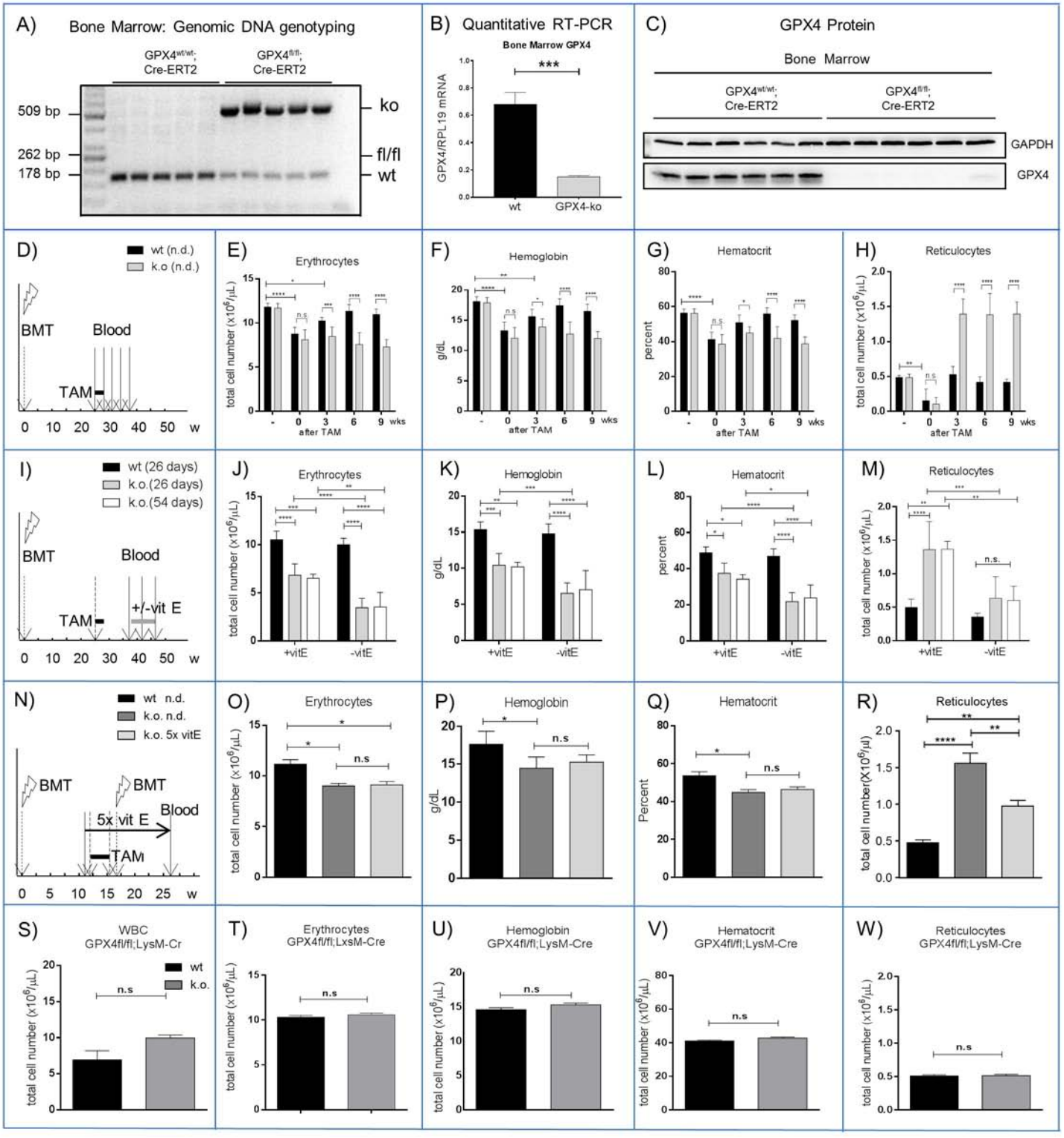
A)
Bone Marrow: Genomic DNA genotyping
GPX4wt/wt; Cre-ERT2
GPX4fl/fl; Cre-ERT2
509 bp
262 bp
178 bp
ko
fl/fl
wt
B)
Quantitative RT-PCR
Bone Marrow GPX4
***
GPX4/RPL19 mRNA
wt
GPX4-ko
C)
GPX4 Protein
Bone Marrow
GPX4wt/wt; Cre-ERT2
GPX4fl/fl; Cre-ERT2
GAPDH
GPX4
D)
wt (n.d.)
k.o (n.d.)
BMT
Blood
TAM
0 10 20 30 40 50 w
E)
Erythrocytes
total cell number (x10^6/µL)
after TAM
F)
Hemoglobin
g/dL
G)
Hematocrit
percent
H)
Reticulocytes
total cell number (x10^6/µL)
I)
wt (26 days)
k.o.(26 days)
k.o.(54 days)
BMT
Blood
TAM
+/-vit E
0 10 20 30 40 50 w
J)
Erythrocytes
+vitE
-vitE
K)
Hemoglobin
L)
Hematocrit
M)
Reticulocytes
n.s.
N)
wt n.d.
k.o. n.d.
k.o. 5x vitE
BMT
BMT
5x vit E
Blood
TAM
0 5 10 15 20 25 w
O)
Erythrocytes
P)
Hemoglobin
Q)
Hematocrit
Percent
R)
Reticulocytes
total cell number(X10^6/µl)
S)
WBC
GPX4fl/fl;LysM-Cr
wt
k.o.
n.s
T)
Erythrocytes
GPX4fl/fl;LxsM-Cre
U)
Hemoglobin
GPX4fl/fl;LysM-Cre
V)
Hematocrit
GPX4fl/fl;LysM-Cre
W)
Reticulocytes
GPX4fl/fl;LysM-Cre

Figure 2

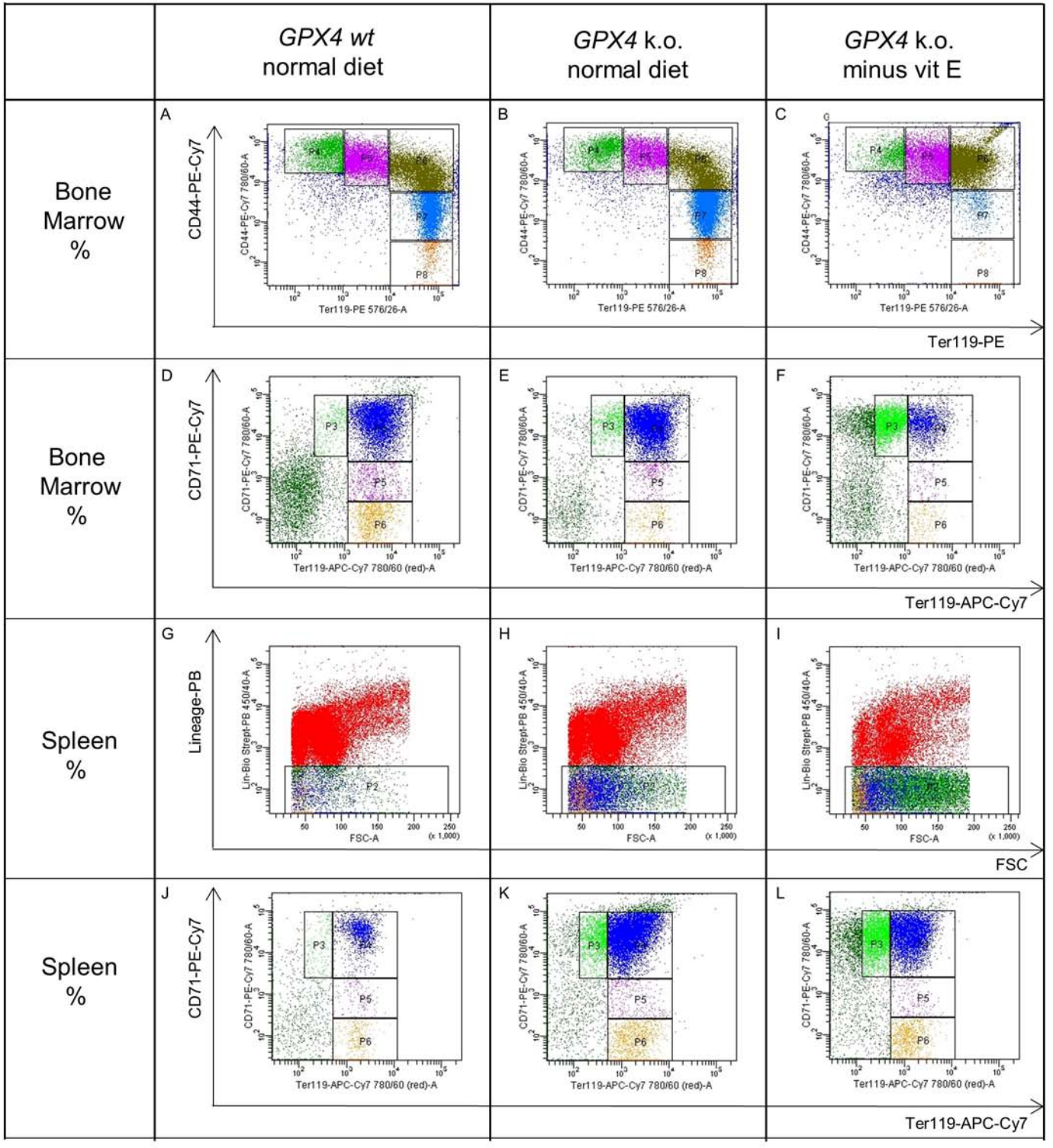
GPX4 wt
normal diet
GPX4 k.o.
normal diet
GPX4 k.o.
minus vit E
Bone Marrow %
Bone Marrow %
Spleen %
Spleen %
A
B
C
D
E
F
G
H
I
J
K
L
CD44-PE-Cy7
CD44-PE-Cy7 780/60-A
Ter119-PE 576/26-A
Ter119-PE
CD71-PE-Cy7
CD71-PE-Cy7 780/60-A
Ter119-APC-Cy7 780/60 (red)-A
Ter119-APC-Cy7
Lineage-PB
Lin-Bio Strept-PB 450/40-A
FSC-A
(x 1,000)
FSC
P1
P2
P3
P4
P5
P6
P7
P8

Figure 3

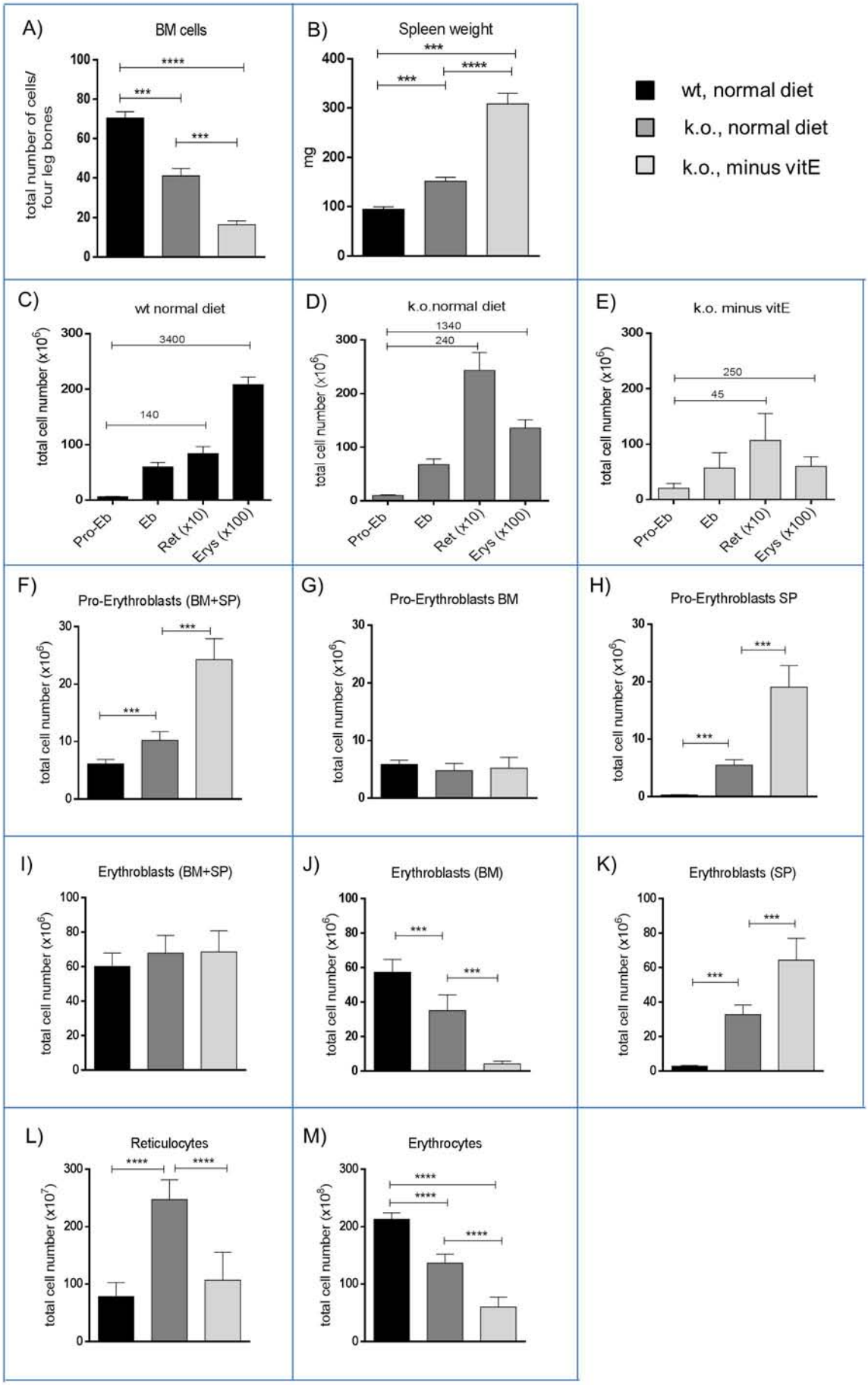
A)
BM cells
total number of cells/ four leg bones
B)
Spleen weight
mg
wt, normal diet
k.o., normal diet
k.o., minus vitE
C)
wt normal diet
total cell number (x10^6)
3400
140
Pro-Eb
Eb
Ret (x10)
Erys (x100)
D)
k.o.normal diet
1340
240
E)
k.o. minus vitE
250
45
F)
Pro-Erythroblasts (BM+SP)
G)
Pro-Erythroblasts BM
H)
Pro-Erythroblasts SP
I)
Erythroblasts (BM+SP)
J)
Erythroblasts (BM)
K)
Erythroblasts (SP)
L)
Reticulocytes
total cell number (x10^7)
M)
Erythrocytes
total cell number (x10^8)

Figure 4

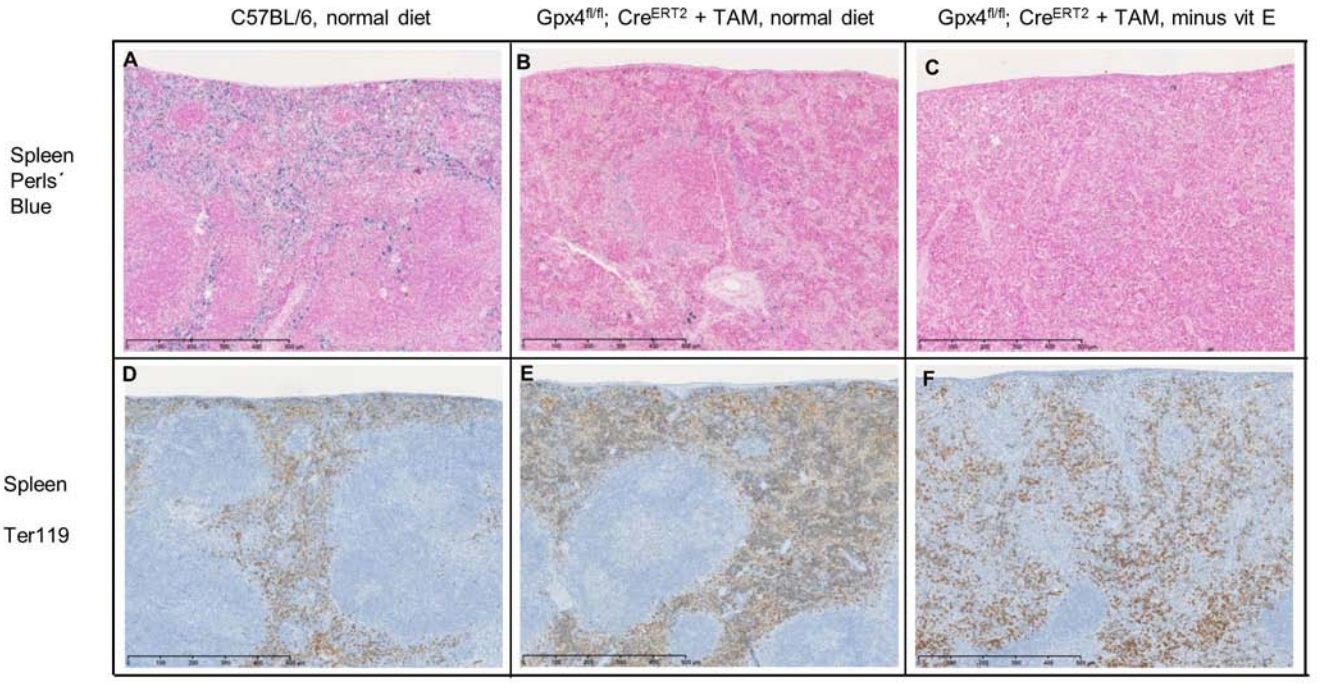
C57BL/6, normal diet
Gpx4fl/fl; CreERT2 + TAM, normal diet
Gpx4fl/fl; CreERT2 + TAM, minus vit E
Spleen Perls´ Blue
Spleen Ter119
A
B
C
D
E
F

Figure 5

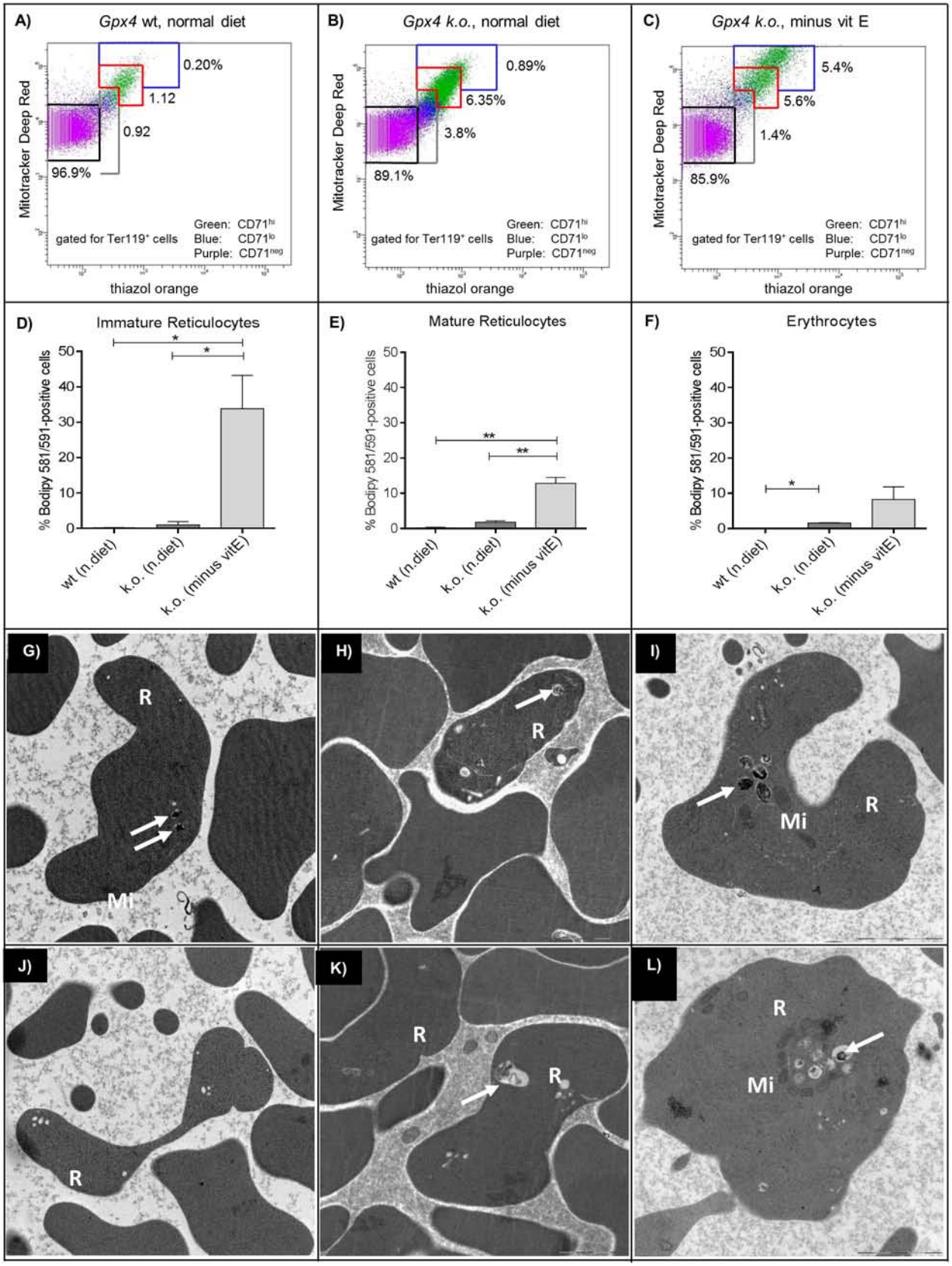
A)
Gpx4 wt, normal diet
0.20%
1.12
0.92
96.9%
Mitotracker Deep Red
thiazol orange
gated for Ter119+ cells
Green: CD71hi
Blue: CD71lo
Purple: CD71neg
B)
Gpx4 k.o., normal diet
0.89%
6.35%
3.8%
89.1%
C)
Gpx4 k.o., minus vit E
5.4%
5.6%
1.4%
85.9%
D)
Immature Reticulocytes
E)
Mature Reticulocytes
F)
Erythrocytes
% Bodipy 581/591-positive cells
wt (n.diet)
k.o. (n.diet)
k.o. (minus vitE)
G)
H)
I)
J)
K)
L)
R
Mi

Figure 6

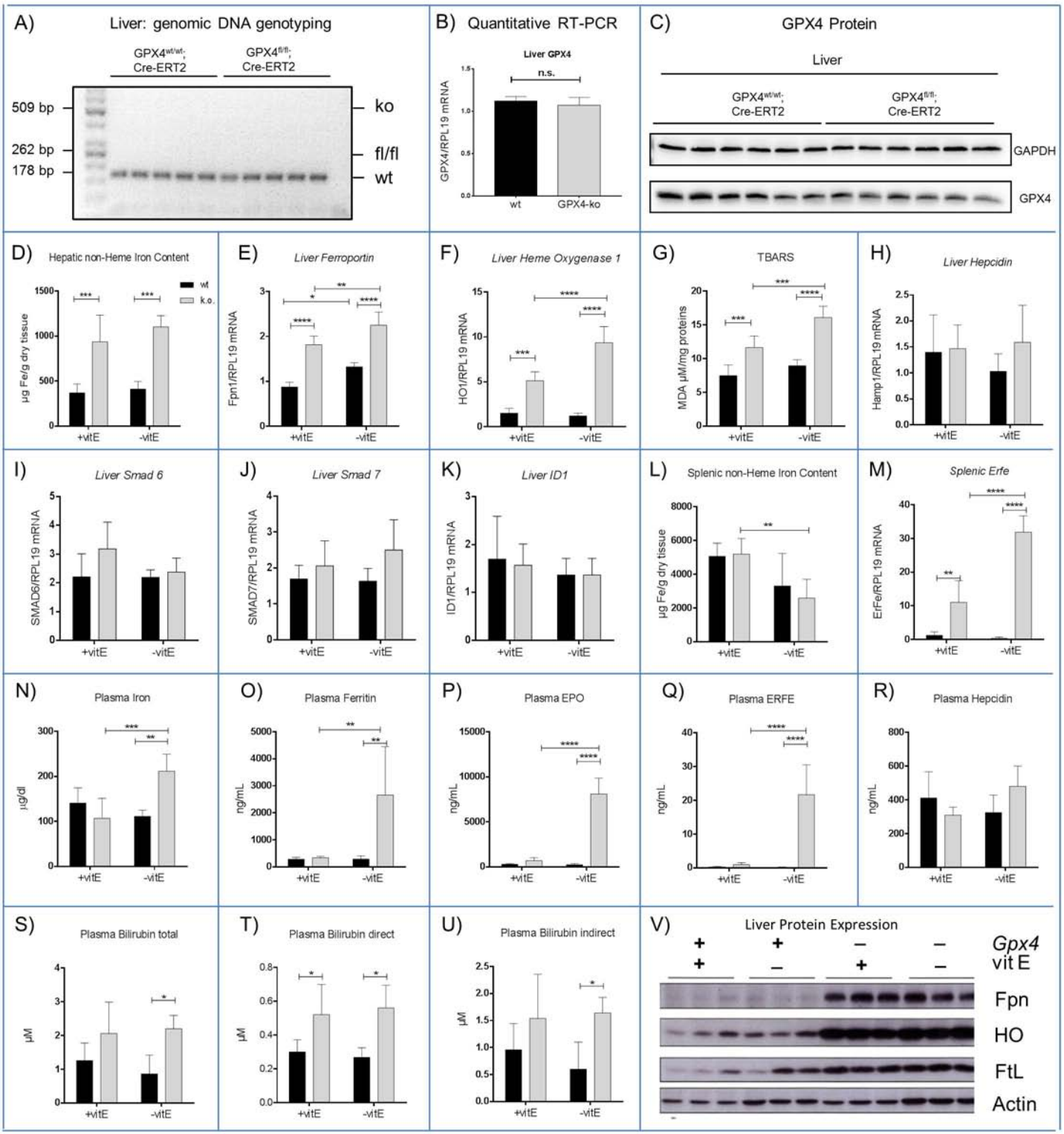
A)
Liver: genomic DNA genotyping
GPX4wt/wt; Cre-ERT2
GPX4fl/fl; Cre-ERT2
509 bp
262 bp
178 bp
ko
fl/fl
wt
B)
Quantitative RT-PCR
Liver GPX4
n.s.
GPX4/RPL19 mRNA
wt
GPX4-ko
C)
GPX4 Protein
Liver
GPX4wt/wt; Cre-ERT2
GPX4fl/fl; Cre-ERT2
GAPDH
GPX4
D)
Hepatic non-Heme Iron Content
wt
k.o.
µg Fe/g dry tissue
+vitE
-vitE
E)
Liver Ferroportin
Fpn1/RPL19 mRNA
F)
Liver Heme Oxygenase 1
HO1/RPL19 mRNA
G)
TBARS
MDA µM/mg proteins
H)
Liver Hepcidin
Hamp1/RPL19 mRNA
I)
Liver Smad 6
SMAD6/RPL19 mRNA
J)
Liver Smad 7
SMAD7/RPL19 mRNA
K)
Liver ID1
ID1/RPL19 mRNA
L)
Splenic non-Heme Iron Content
µg Fe/g dry tissue
M)
Splenic Erfe
EtFe/RPL19 mRNA
N)
Plasma Iron
µg/dl
O)
Plasma Ferritin
ng/mL
P)
Plasma EPO
ng/mL
Q)
Plasma ERFE
ng/mL
R)
Plasma Hepcidin
ng/mL
S)
Plasma Bilirubin total
µM
T)
Plasma Bilirubin direct
µM
U)
Plasma Bilirubin indirect
µM
V)
Liver Protein Expression
Gpx4
vit E
Fpn
HO
FtL
Actin

Figure 7

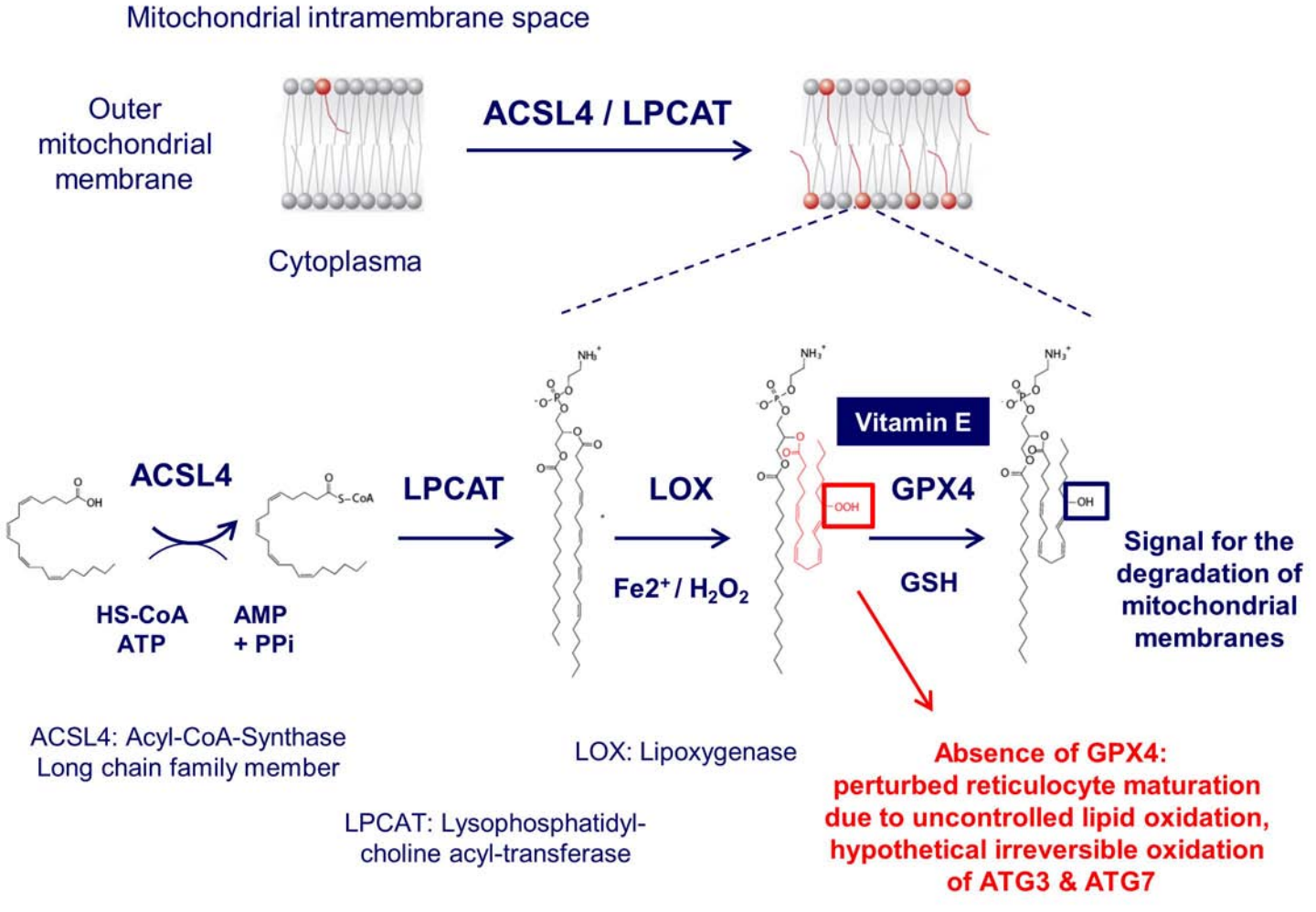
Mitochondrial intramembrane space
Outer mitochondrial membrane
ACSL4 / LPCAT
Cytoplasma
ACSL4
LPCAT
LOX
Vitamin E
GPX4
Fe2+ / H2O2
GSH
HS-CoA
ATP
AMP
+ PPi
Signal for the degradation of mitochondrial membranes
ACSL4: Acyl-CoA-Synthase Long chain family member
LOX: Lipoxygenase
LPCAT: Lysophosphatidyl-choline acyl-transferase
Absence of GPX4: perturbed reticulocyte maturation due to uncontrolled lipid oxidation, hypothetical irreversible oxidation of ATG3 & ATG7

Supplementary Information

Antibodies for FACS analysis

Antigen-Conjugate	Company	Clone	Concentration
CD44-PE-Cy7	eBiosciences	IM7	0.3µg/50µL
CD71-PE-Cy7	Biolegend	R17217	0.3µg/50µL
Ter119-PE	eBiosciences	Ter119	0.3µg/50µL
Ter119-APC-Cy7	eBiosciences	Ter119	0.3µg/50µL
CD16/32	BD Biosciences	2.4G2	0.5µg/50µL
CD3e-biotin	eBiosciences	145-2C11	0.5µg/50µL
CD11b-biotin	eBiosciences	M1/70	0.5µg/50µL
CD19-biotin	eBiosciences	1D3	0.5µg/50µL
B220-biotin	eBiosciences	RA3-682	0.5µg/50µL
GR-1-biotin	eBiosciences	RB5-8C5	0.5µg/50µL
CD45-BV785	Biolegend	30-F11	0.01µg/50µL
CD11b-PerCP-Cy5.5	Biolegend	M1/70	0.01µg/50µL
F4/80-BV421	Biolegend	BM8	0.08µg/50µL
CD11c-BV605	Biolegend	N418	0.02µg/50µL
VCAM1-FITC	eBiosciences	429	0.125µg/50µL
MHCII-BV510	Biolegend	M5/114.15.2	0.06µg/50µL
Ly6C-APC	Biolegend	HK1.4	0.005µg/50µL

Antibodies for Western-blotting

Protein	Company	Cat nr	Dilution
GPX4	ABCAM	125066	1:1000
Fpn	Alpha Diagnostics	MTP11-A	1:1000
HO1	Enzo Life Sciences	ADI-SPA-896-F	1:500
FtL	Santa Cruz	sc-14420	1:250
Actin	Sigma	A1978	1:10000

Primers for monitoring deletion of the GPX4 gene

	Primer forward	Primer reverse
floxed vs wt	ACTCCCCGTGGAACTGTGAGCTTTGTGC	GGATCTAAGGATCACCAGAGCTGAGGCTGC
deleted	GTGTACCACGTAGGTACAGTGTCTGC	GGATCTAAGGATCACCAGAGCTGAGGCTGC

Primers for quantitative RT-PCR

	Primer forward	Primer reverse
GPX4	CGCTCCATGCACGAATTCTC	GCACACGAAACCCCTGTACT
Fpn	TGTCAGCCTGCTGTTTGCAGGA	TCTTGCAGCAACTGTGTCACCG
Hepcidin	ATACCAATGCAGAAGAGAAGG	AACAGATACCACACTGGGAA
SMAD6	GTTGCAACCCCACTTC	GGAGGAGACAAGAATA
SMAD7	GCAGGCTGTCCAGATGCTGT	GATCCCCAGGCTCCAGAAGA
ID1	ACCCTGAACGGCGAGATCA	TCGTCGGCTGGAACACATG
HO-1	AGGCTAAGACCGCCTTCCT	TGTGTTCCTCTGTCAGCATCA
Erfe	AGCGAGCTCTTCACCATCTC	TGTCCAAGAAGACAGAAGTGTAGTG
RPL19	AGGCATATGGGCATAGGGAAGAG	TTGACCTTCAGGTACAGGCTGTG
Fpn	TGTCAGCCTGCTGTTTGCAGGA	TCTTGCAGCAACTGTGTCACCG
Hepcidin	ATACCAATGCAGAAGAGAAGG	AACAGATACCACACTGGGAA
SMAD6	GTTGCAACCCCACTTC	GGAGGAGACAAGAATA
SMAD7	GCAGGCTGTCCAGATGCTGT	GATCCCCAGGCTCCAGAAGA
ID1	ACCCTGAACGGCGAGATCA	TCGTCGGCTGGAACACATG
HO-1	AGGCTAAGACCGCCTTCCT	TGTGTTCCTCTGTCAGCATCA
Erfe	AGCGAGCTCTTCACCATCTC	TGTCCAAGAAGACAGAAGTGTAGTG
RPL19	AGGCATATGGGCATAGGGAAGAG	TTGACCTTCAGGTACAGGCTGTG

Staining of spleen red pulp macrophages (RPM) and bone marrow erythroblastic island macrophages (BMEIM) in GPX4$^{fl/fl}$;LysM-Cre mice

Spleens were cut into small pieces, then digested for 30 min at 37 °C with 2 mg/ml of type IV collagenase (Worthington) and 50U/ml DNase I (Sigma) and passed through a 70-µm cell strainer. Bone marrow was flushed from femur and tibia from mouse hindlimb and passed through a 70-µm cell strainer. Erythrocytes were lysed with ACK (ammonium chloride–potassium bicarbonate) buffer. Dead cells were gated out with use of the live-dead marker eFluor780 (eBioscience). FcγIII/II receptors were blocked by incubation with anti-CD16/32 antibody for 15 min on ice. Cells were washed and incubated with 0.01µg CD45-BV785, 0.01µg CD11b-PerCP-Cy5.5, 0.08µg F4/80-BV421, 0.02µg CD11c-BV605, 0.125µg VCAM1-FITC, 0.06µg MHCII-BV510, and 0.005µg Ly6C-APC antibodies. Cells were analysed on LSR Fortessa (Becton Dickinson).

Transmission Electron microscopy

Blood pellets were fixed in 2.5% electron microscopy grade glutaraldehyde in 0.1 M sodium cacodylate buffer pH 7.4 (Science Services, Munich, Germany), postfixed in 2% aqueous osmium tetraoxide,[1] dehydrated in gradual ethanol (30–100%) and propylene oxide, embedded in Epon (Merck, Darmstadt, Germany) and cured for 24 hours at 60°C. Semithin sections were cut and stained with toluidine blue. Ultrathin sections of 50 nm were collected onto 200 mesh copper grids, stained with uranyl acetate and lead citrate before examination by transmission electron microscopy (Zeiss Libra 120 Plus, Carl Zeiss NTS GmbH, Oberkochen, Germany). Pictures were acquired using a Slow Scan CCD-camera and iTEM software (Olympus Soft Imaging Solutions, Münster, Germany).

Determining the maturation state of reticulocytes

Peripheral blood cells were washed with PBS containing 1 mM EDTA and 2% FCS, filtered through a 40 µm cell strainer (BD Falcon) and incubated with 0.5 µg anti-CD16/32 antibody (clone 2.4G2, BD Bioscience) in 50 µl PBS for 30 min on ice. Cells were stained with 0.3 µg CD71-PE-Cy7, 0.3 µg Ter119-PE or Ter119-APC-Cy7 antibodies for another 30 minutes as well as with Mitotracker Deep Red (MTDR) (Thermo Fisher) and Thiazol Orange (TO)(Biomol) in 50 µL PBS according to the manufacturer's instructions. Mature reticulocytes are defined by CD71 and Ter119 staining as enucleated CD71^{low}/Ter119^{high} cells. CD71^{high}/TEr119^{high} reticulocytes are divided into immature and highly immature reticulocytes based on MTDR and TO staining.

Determining the total number of proerythroblasts and erythroblasts in the bone marrow and spleen and of erythrocytes and reticulocytes in the blood

The percentual fractions of proerythroblasts ($CD71^{high}$, $Ter119^{low}$) and erythroblasts ($CD71^{high-low}$, $Ter119^{high}$) in the bone marrow and spleen were determined by FACS analysis as exemplified in Fig.2. Based on the percentual fractions the total number of erythroid precursors in the bone marrow was assessed by counting absolute cell numbers in the four hindlimb bones and extrapolating the values obtained from wt mice to the known bone marrow cellularity of adult female C57BL/6 wt mice ($466x10^6$ cells).[2] The total number of erythroid precursor cells in the spleen was calculated based on the percentual fraction of erythroid precursor cells in the spleen and the assumption that 100 mg spleen tissue contains 10^8 nucleated cells. The total number of erythrocytes and reticulocytes was assessed based on the fact that 7.8 to 8.0% of the body weight of adult female C57BL/6 mice is blood.[3]

Histology

Histology was done following standard procedures.[4] Immunohistochemistry was performed in a Ventana immunostainer from Roche diagnostics according to manufacturer's instructions.

Western-blot

Protein lysates were obtained by homogenizing snap-frozen tissues in RIPA or LCW buffer supplemented with protease and phosphatase inhibitors (Roche).[5] Protein concentration was determined using the DC protein assay (BioRad). 50µg of total protein and β-actin (Actin) as normalizer were subjected to Western-blot analysis. Western-blot images were acquired on X-ray films and different exposures scanned for quantification.

Genomic DNA PCR, RNA Extraction, reverse transcription and qRT-PCR

Deletion of the *GPX4* gene was analysed using two PCR reactions: the first reaction (primer pair oligoGPX4I5f1/ oligoPFrev1, annealing 65.5°C, elongation for 60 sec) detects the deleted allele (509 bp), whereas the second reaction (primer pair oligoPFf1/oligoPFrev1, annealing 68°C, elongation 30 sec) discriminates between the floxed (262 bp) and the wt allele (178 bp). Both PCR reactions were pooled for gel electrophoresis. Incomplete deletion of *GPX4* is detected by the presence of the floxed allele. RNA was isolated from tissues using the Trizol reagent (Life technologies) and TissueLyser homogenizer (Qiagen), reverse-transcribed and used in SYBR green qRT-PCR as described.[6] mRNA expression was calculated relative to RPL19. Data were analyzed using the ΔΔCt method.[7]

Plasma and liver biochemistry and tissue iron measurement

Plasma iron concentration was assessed using the SFBC colorimetric kit (Biolabo, Maizy, France). Plasma ferritine and bilirubin were measured using the Olympus AU400 analyzer at the Claude Bernard Institute (Paris, France). Tissue non-heme iron content was measured using the bathophenanthroline method and calculated against dry weight tissue.[8] Hepatic lipid peroxidation was assessed on 0.05g hepatic tissue using the thiobarbituric acid assay (TBARS).[9]

Plasma hepcidin, erythropoietin (EPO) and erythroferrone (ERFE) measurement

Plasma hepcidin and EPO concentrations were measured using the "Hepcidin Murine-Compete ELISA Kit" (Intrinsic Lifescience, USA) and the "Mouse erythropoietin quantikine ELISA kit" (R&D systems) according to manufacturer's instructions. Mouse ERFE was measured in a custom ELISA using monoclonal antibodies and recombinant mouse ERFE standards, kindly donated by Silarus Therapeutics (La Jolla, CA, USA), as described.[10] Concentrations were extrapolated against a standard curve using the GraphPad Prism software.

Statistical analyses

Figures were generated and statistical analyses performed by using GraphPad Prism software (Version 6.01 for Windows). Normality test (Shapiro-Wilk test) and Bartlett's test of homogeneity variances and two-way ANOVA with no assumption of homogeneity of variance (with Sidak's test of multiple comparisons) were used to calculate statistical significances unless otherwise stated in the figure legends. Differences with p values less than 0.05 were considered to be statistically significant (* $p<0.05$; ** $p<0.001$; *** $p<0.0001$; **** $p<0.0001$). Values mentioned are Mean ± SEM.

Legends to Supplementary Figures

Supplementary Figure 1:

Cre activation induces an aplastic anemia in mice with *GPX4*-deficient as well as *GPX4*-proficient hematopoietic system. Scheme of the wt and gene-modified murine GPX4 locus before and after Cre activation. White and black triangles represent loxP and frt sites, respectively (A). Lethally irradiated mice reconstituted with BM cells from *GPX4*$^{fl/fl}$*;CreERT2* or *GPX4*$^{wt/wt}$*;CreERT2* donor mice were fed a tamoxifen citrate containing diet for three weeks to delete *GPX4*. EDTA-blood was collected from the tail vein before (left columns, - TAM) and at the last day of tamoxifen administration (right columns, + TAM), and subjected to the analysis of blood parameters (mice harboring *GPX4* in the bone marrow, designated wt, black columns, n=7, and mice lacking *GPX4* in the bone marrow, designated ko, grey columns, n=22). Red blood counts (RBC, B), hemoglobin (HGB, C), hematocrit (HCT,D), mean corpuscular volume (MCV, E) reticulocyte counts (F) , platelet counts (G), mean platelet volume (MPV, H), platelet width distribution (PDW, I), platelet large cell fraction (P-LCR, J), platelet crit (PCT, K), white blood counts (WBC, L), neutrophils (M), lymphocytes (N), monocytes (O), and eosinophils (P) were determined. For reticulocytes (F) and eosinophils (P) that did not pass the Shapiro-Wilk normality test, non-parametric ANOVA with Dunn's multiple comparison test was applied. The decrease in lymphocyte and monocyte counts induced by Cre activation in control mice is further significantly enhanced by *GPX4*-deficiency in the hematopoietic system. The increase in platelet indices PMV, PDW and P-LCR is presumably a transient response to toxic platelet activation.[11]

Supplementary Figure 2:

Additional red blood cell parameters to the experiments shown in Fig. 1D-H and I-M. The temporal schemes in A and F are identical to the schemes in Fig. 1D and I. Mean cell volume (MCV) (B and G), mean cell hemoglobin (MCH) (C and H), mean cell hemoglobin concentration (MCHC) (D and I), and red blood cell distribution width (RDW-SD) (E and J). Number of mice and designations as in Fig.1. MCV, MCH and RDW-SD are significantly increased in mice with a *GPX4*-deficient hematopoietic system. Vitamin E depletion further aggravates the phenotype (G,H,J).

Supplementary Figure 3:

The erythropenic phenotype induced by *GPX4* deficiency in the hematopoietic system is stably transmitted in two consecutive rounds of bone marrow transplantation. Experimental design and temporal scheme (A). Lethally irradiated wt mice were reconstituted with 10^6 BM cells of *GPX4*$^{fl/fl}$*;Cre-ERT2* mice (1st transplantation) and allowed to recover for 12 weeks before a tamoxifen citrate containing diet was administered for three weeks. Three mice of the same 1st transplantation group were not treated with tamoxifen and served as control donors for the 2nd transplantation. Two weeks after terminating the tamoxifen containing diet, 10^6 bone marrow cells of mice that had received the tamoxifen containing diet (grey bars, designated + TAM, n=5) and of control mice that had not received tamoxifen (black bars, designated – TAM, n=5) were injected into lethally irradiated wt mice (2nd transplantation). 20 weeks after the 2nd transplantation, 10^6 *GPX4*-deficient (n=10) and *GPX4*- proficient BM cells (n=6) of the recipients of the 2nd transplantation were injected into lethally irradiated wt mice (3rd transplantation). Blood was drawn 11 weeks after the second and 11 weeks after the third transplantation. The erythropenic phenotype was stably transmitted after deletion of *GPX4* in the hematopoietic system in two consecutive rounds of BM transplantation (2nd and 3rd transplantation)(B, C, D, E, I), whereas alterations in the white blood counts and platelet indices were not consistently observed after the 2nd and 3rd transplantation (J-O).

Supplementary Figure 4:

Minor differences in the development of red pulp and and bone marrow erythroblastic island macrophages in GPX4$^{fl/fl}$;LysM-Cre mice. Representative FACS plots showing gating strategy for red pulp macrophages (RPM, A, n=3) and bone marrow erythroblastic island macrophages (BMEIM, B, n=3) for *GPX4*$^{fl/fl}$*;LysM-Cre* and *GPX*$^{fl/fl}$ mice. Cell counts, frequencies of CD45-positive cells for RPM (upper panel) and BMEIM (lower panel) supplemented with total counts for spleen and bone marrow cells are shown in C. The significance was calculated with unpaired two-tailed Student's t-test.

Supplementary Figure 5:

Erythropoiesis is not affected by vitamin E depletion in wt mice. Three weeks old female wt mice were fed either a normal (black columns, designated + vitE, n=10) or a vitamin E-depleted diet (grey columns, designated – vitE, n=9) upon weaning. Blood was

drawn 17 weeks after starting the vitamin E depleted diet (A). In wt mice red blood parameters were not affected by vitamin E depletion in the diet (B-I).

Supplementary Figure 6:

Reticulocyte maturation is impaired by *GPX4*-deficiency in the hematopoietic system and the phenotype is strongly aggravated by concomitant vitamin E depletion. Total numbers of mature, immature, and highly immature reticulocytes in wt mice maintained on a normal diet (A, n=4) and in mice with *GPX4*-deficient hematopoiesis kept either on a normal (B, n=4) or vitamin E-depleted diet (C, n=6). The FACS staining of blood cells of one representative mouse of each group is shown in Fig. 5A-C. Mature reticulocytes were defined by $CD71^{low}$/$Ter119^{high}$ staining. $CD71^{high}$/$Ter119^{high}$ cells were divided into immature and highly immature reticulocytes based on Mitotracker Deep Red (MTDR) and thiazol orange (TO) staining. The total numbers of reticulocytes of the various stages of maturation were determined based on the percentual fraction of mature, immature and highly immature reticulocytes, the reticulocyte counts per µL obtained by Sysmex analysis, and the mean total blood content (7.8 to 8.0 % of body weight) of adult female C57BL/6 mice.[3] The significance was calculated by Mann-Whitney test. To visualize and quantify the differences in each fraction of reticulocytes under the different conditions, data of A, B, and C were replotted in D, E, and F. Deletion of *GPX4* in hematopoietic cells of mice kept on a normal diet caused an increase in all fractions of reticulocytes (D-F). The differentially higher increase in more immature cells resulted in a general shift towards more immature reticulocytes (G-I). Under combined *GPX4*- and vitamin E-deficiency, production of reticulocytes did not keep up with the severity of the erythropenia and the production of proerythroblasts in the spleen, i.e. total reticulocyte counts were not increased to a significant extent compared to wt mice despite the strong decrease in RBC, hemoglobin and hematocrit. The absolute numbers as well as the percentage of highly immature reticulocytes were increased in these mice at the expense of mature reticulocytes (C,F,I).

Supplementary Figure 7:

Ferroportin expression in the duodenum and hemoxygenase-1 expression in the liver. Unaltered ferroportin (Fpn) expression in mice with GPX4-deficient hematopoiesis (A). Quantification of hemoxygenase-1 expression in the liver of mice with GPX4-deficiency in the hematopoietic system (B).

Supplementary References

1. Wood RL, Luft JH. The Influence of Buffer Systems on Fixation with Osmium Tetroxide. J Ultrastruct Res. 1965;12:22-45.
2. Colvin GA, Lambert JF, Abedi M, et al. Murine marrow cellularity and the concept of stem cell competition: geographic and quantitative determinants in stem cell biology. Leukemia. 2004;18(3):575-583.
3. Harkness JE, American College of Laboratory Animal M. Harkness and Wagner's biology and medicine of rabbits and rodents. Oxford: Wiley-Blackwell, 2010.
4. Suvarna SK. Bancroft's theory and practice of histological techniques / Kim S Suvarna, Christopher Layton, John D. Bancroft. Kidlington: Elsevier, 2018.
5. Ingold I, Berndt C, Schmitt S, et al. Selenium Utilization by GPX4 Is Required to Prevent Hydroperoxide-Induced Ferroptosis. Cell. 2018;172(3):409-422.
6. Altamura S, D'Alessio F, Selle B, Muckenthaler MU. A novel TMPRSS6 mutation that prevents protease auto-activation causes IRIDA. The Biochemical journal. 2010;431(3):363-371.
7. Livak KJ, Schmittgen TD. Analysis of Relative Gene Expression Data Using Real-Time Quantitative PCR and the 2-[Delta][Delta]CT Method. Methods. 2001;25(4):402-408.
8. Torrance JD, Bothwell TH. A simple technique for measuring storage iron concentrations in formalinised liver samples. S Afr J Med Sci. 1968;33(1):9-11.
9. Ohkawa H, Ohishi N, Yagi K. Assay for lipid peroxides in animal tissues by thiobarbituric acid reaction. Analytical biochemistry. 1979;95(2):351-358.
10. Kautz L, Jung G, Du X, et al. Erythroferrone contributes to hepcidin suppression and iron overload in a mouse model of beta-thalassemia. Blood. 2015;126(17):2031-2037.
11. Jindal S, Gupta S, Gupta R, et al. Platelet indices in diabetes mellitus: indicators of diabetic microvascular complications. Hematology. 2011;16(2):86-89.

Supplementary Figure 1

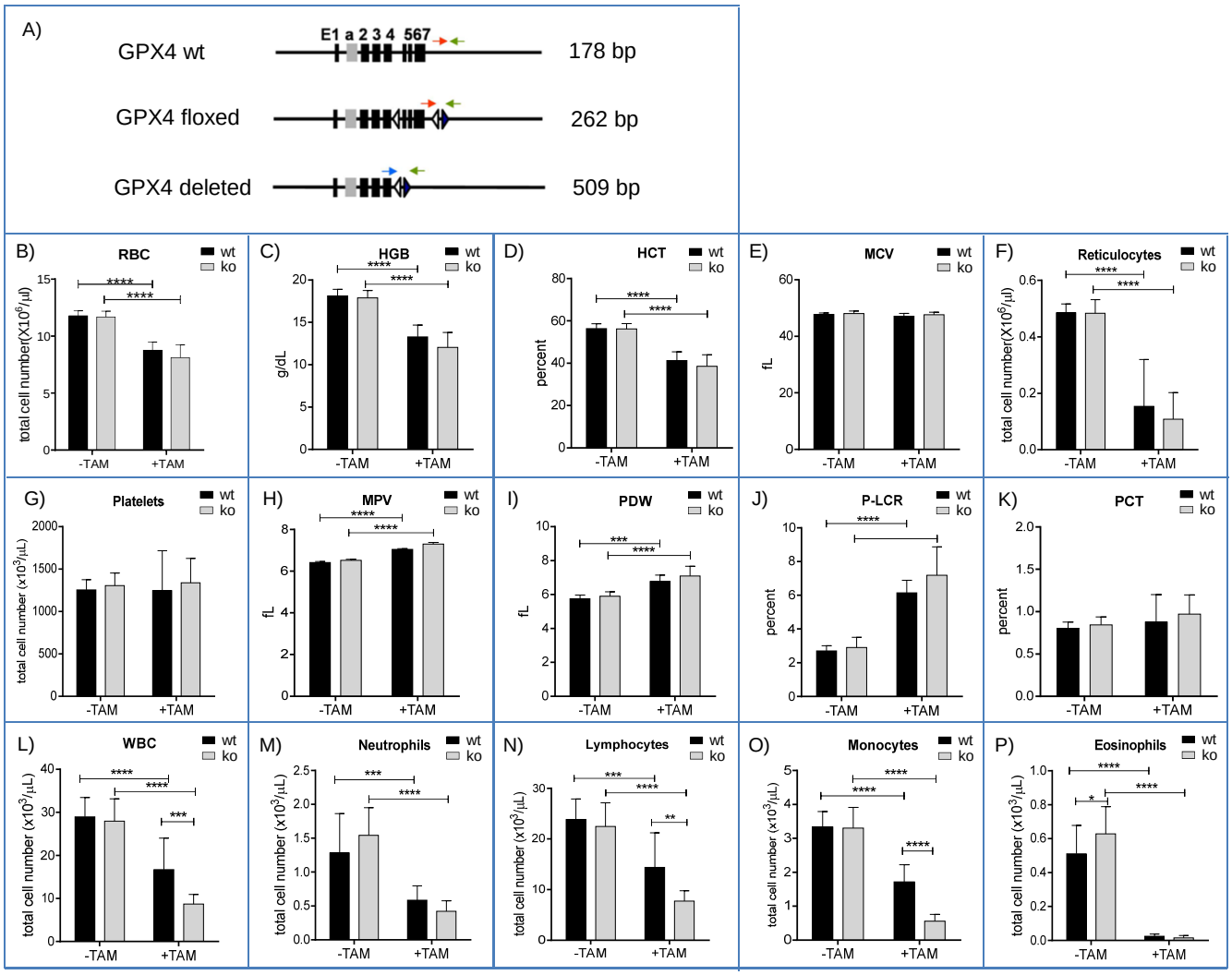

Supplementary Figure 2

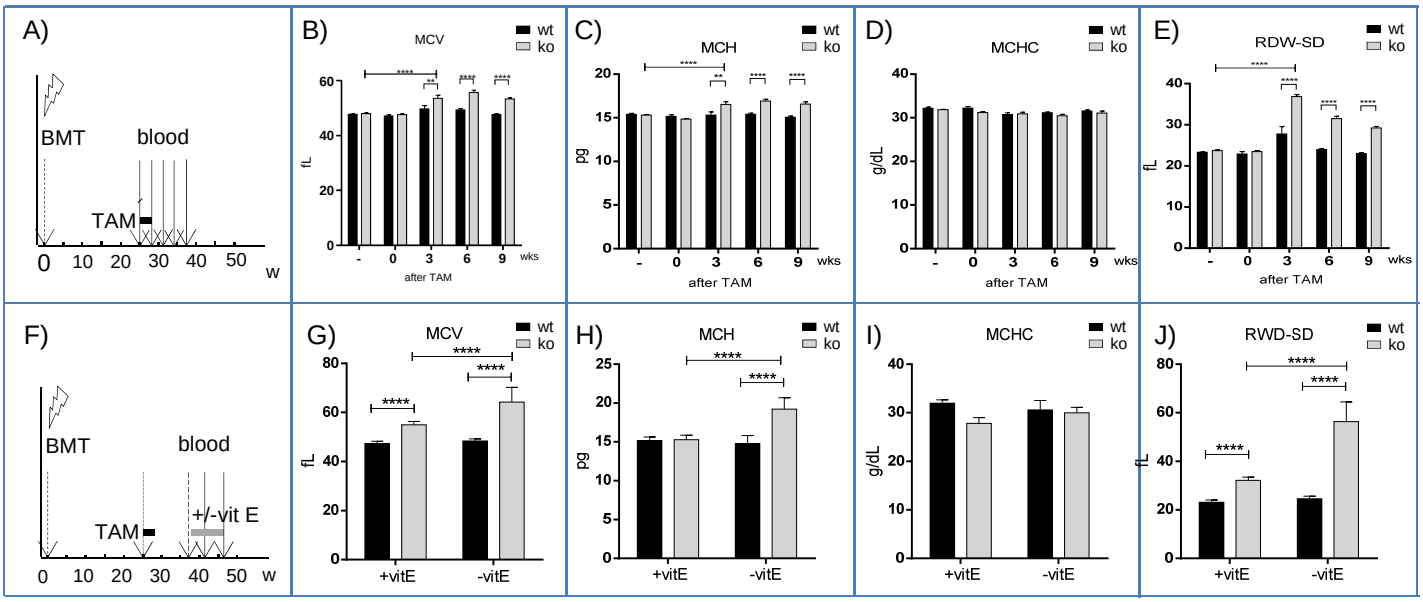

Supplementary Figure 3

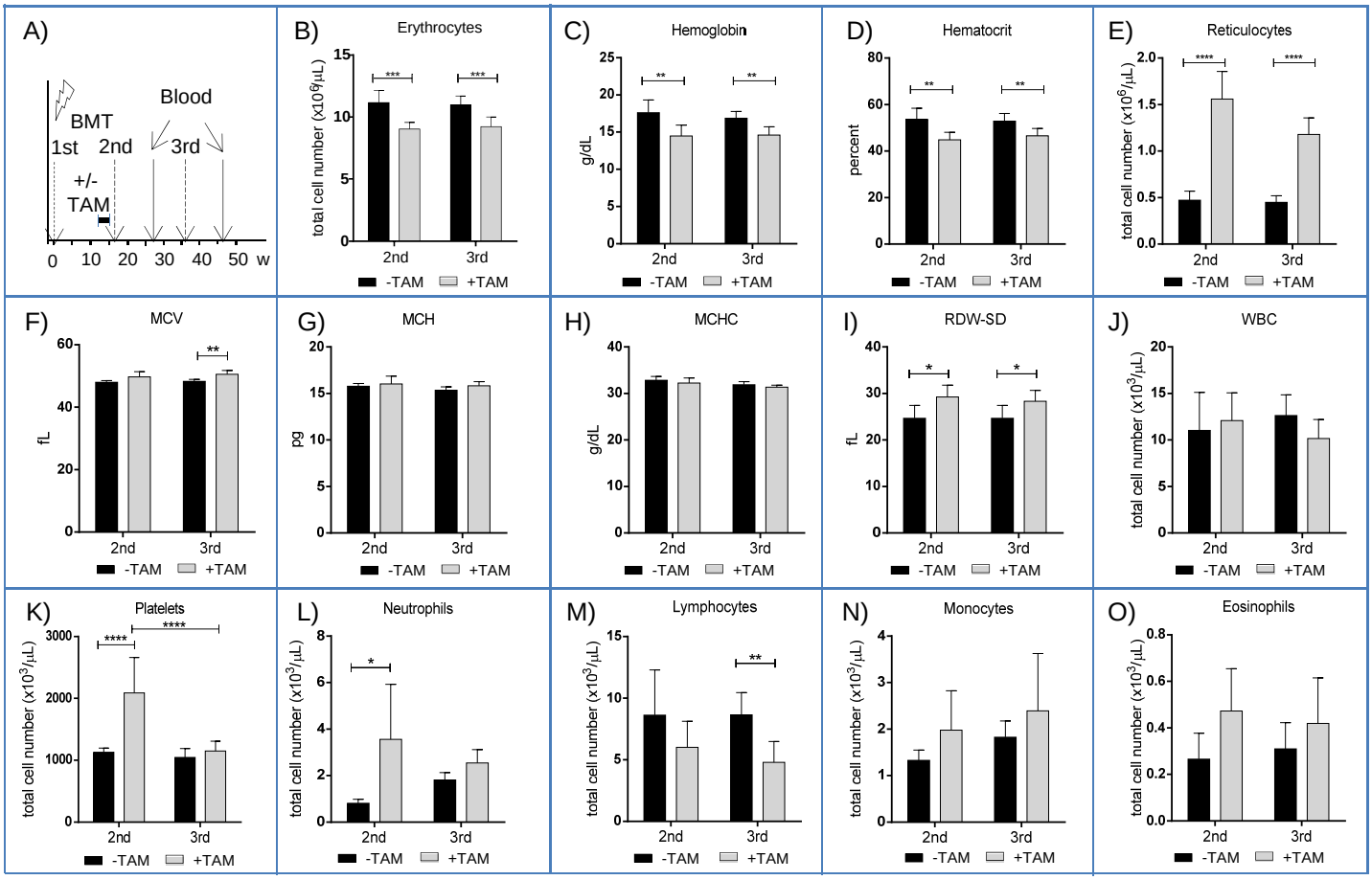

Supplementary Figure 4

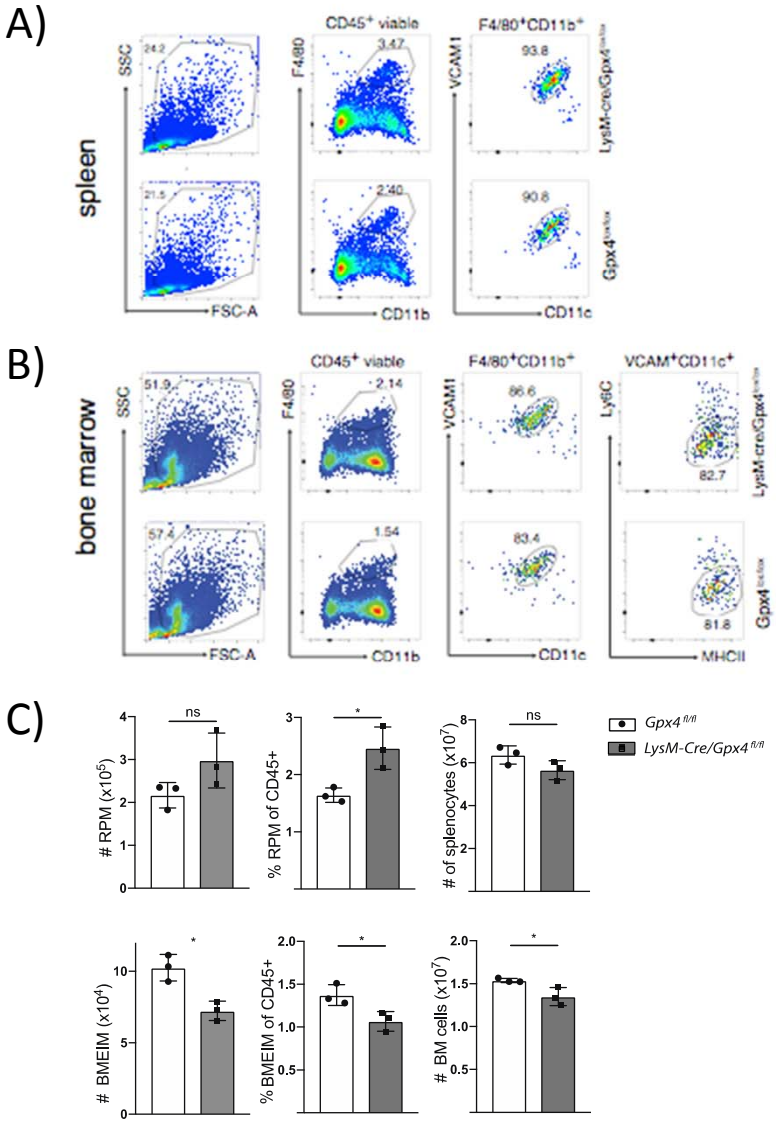

Supplementary Figure 5

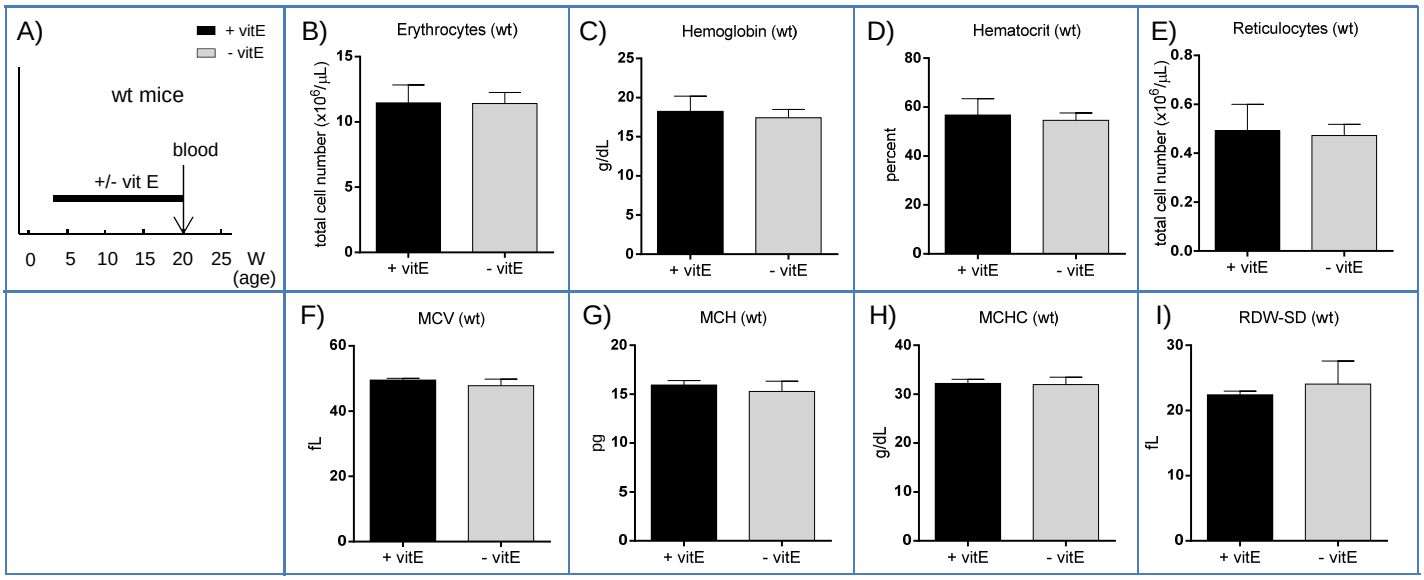

Supplementary Figure 6

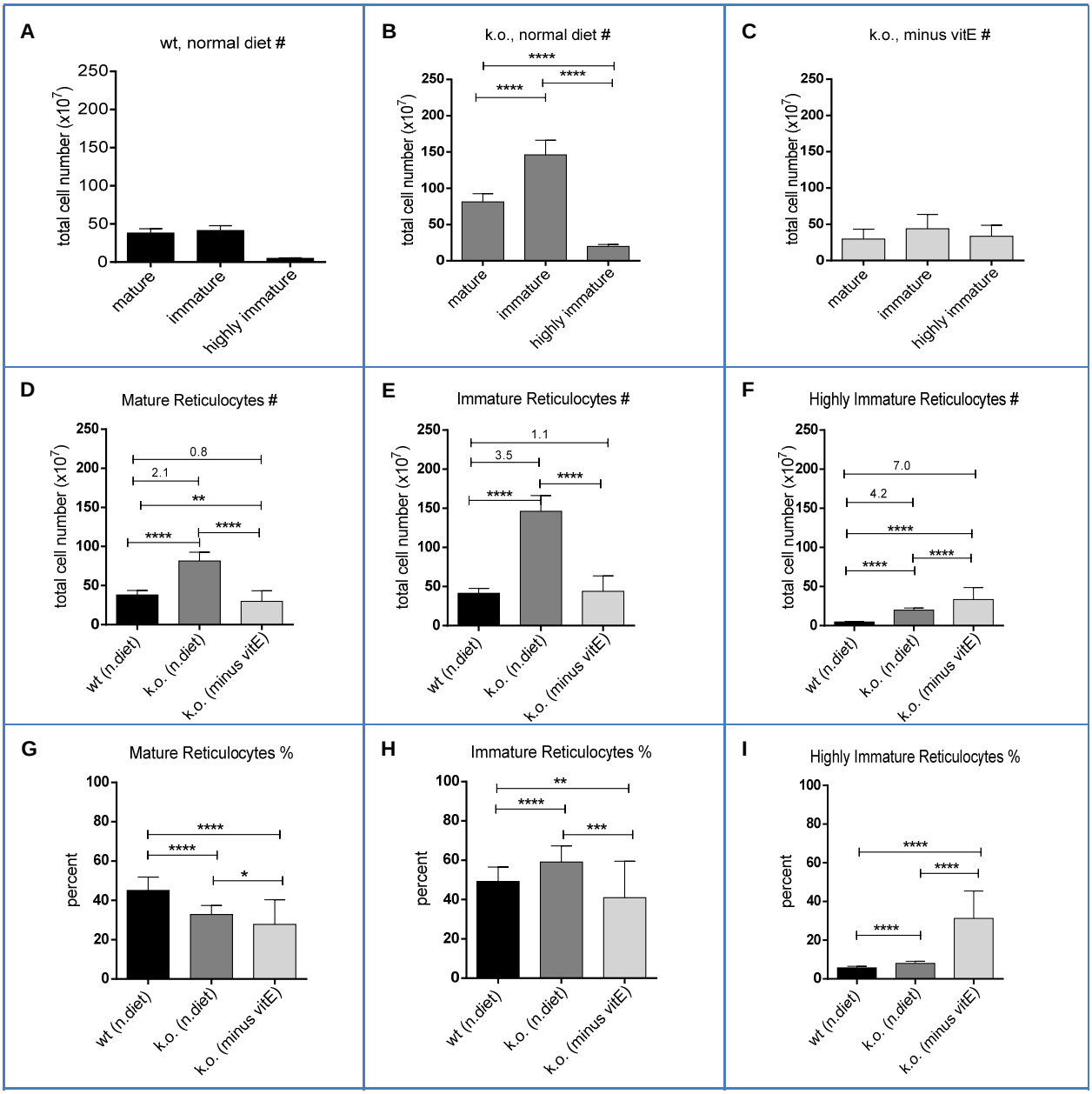

Supplementary Figure 7